



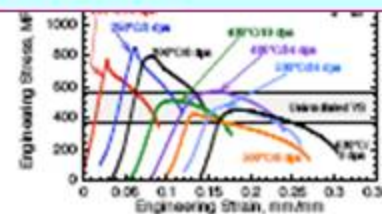
Multi-scale approach in modeling of radiation induced phenomena in irradiated materials

Alexander Ryazanov

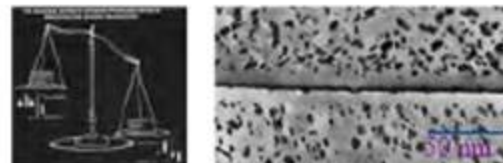
**Joint ICTP/IAEA Advanced Workshop on Development of
Radiation Resistant Materials**

Main Physical Phenomena of Radiation Resistance in Fusion Structural Materials

- Radiation hardening and embrittlement ($<0.4 T_M$, >0.1 dpa)



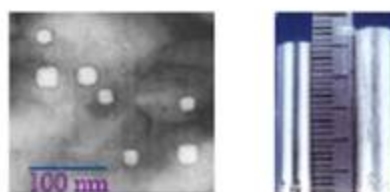
- Phase instabilities from radiation-induced precipitation ($0.3-0.6 T_M$, >10 dpa)



- Irradiation creep ($<0.45 T_M$, >10 dpa)



- Volumetric swelling from void formation ($0.3-0.6 T_M$, >10 dpa)



- High temperature He embrittlement ($>0.5 T_M$, >10 dpa)



Materials for Fission and Fusion Reactors

- **Graphite Materials :**
Graphite, C-C composites
- **Metallic Materials:**
Austenitic Steels, Ferritic – martensitic Steels, ODS materials, V-alloys
- **Ceramic Materials:**
SiC – composites, Al₂O₃, MgO, ZrO₂

Schematic diagram: relevant phenomena and computational methods

Phenomena

single displacement cascade

multiple cascades,
cascade overlap

defect and solute
migration and clustering

void swelling, hardening,
embrittlement, creep, stress
corrosion cracking, ...

collisional phase

annealing phase

defect/solute
diffusion

microstructure
evolution

quenching

mechanical
property
changes

10^{-14} s

10^{-11} s

10^{-8} s

10^1 s

10^4 s

$>10^6$ s

molecular dynamics

ab initio

kinetic Monte Carlo

MD dislocation dynamics

finite element

reaction rate theory, phase field

3D dislocation dynamics

Methods

10^{-9} m

10^{-7} m

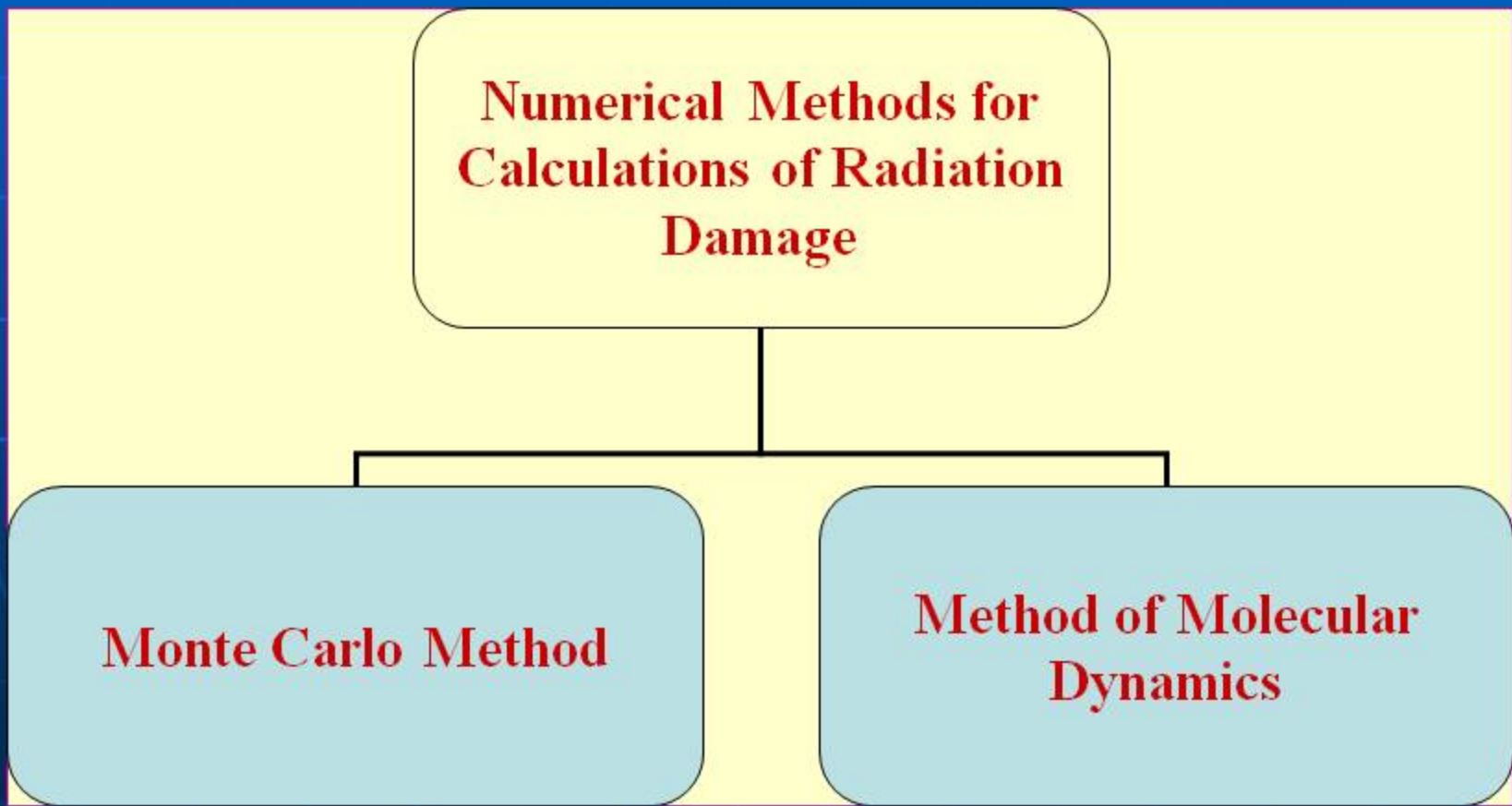
10^{-6} m

$>10^{-3}$ m

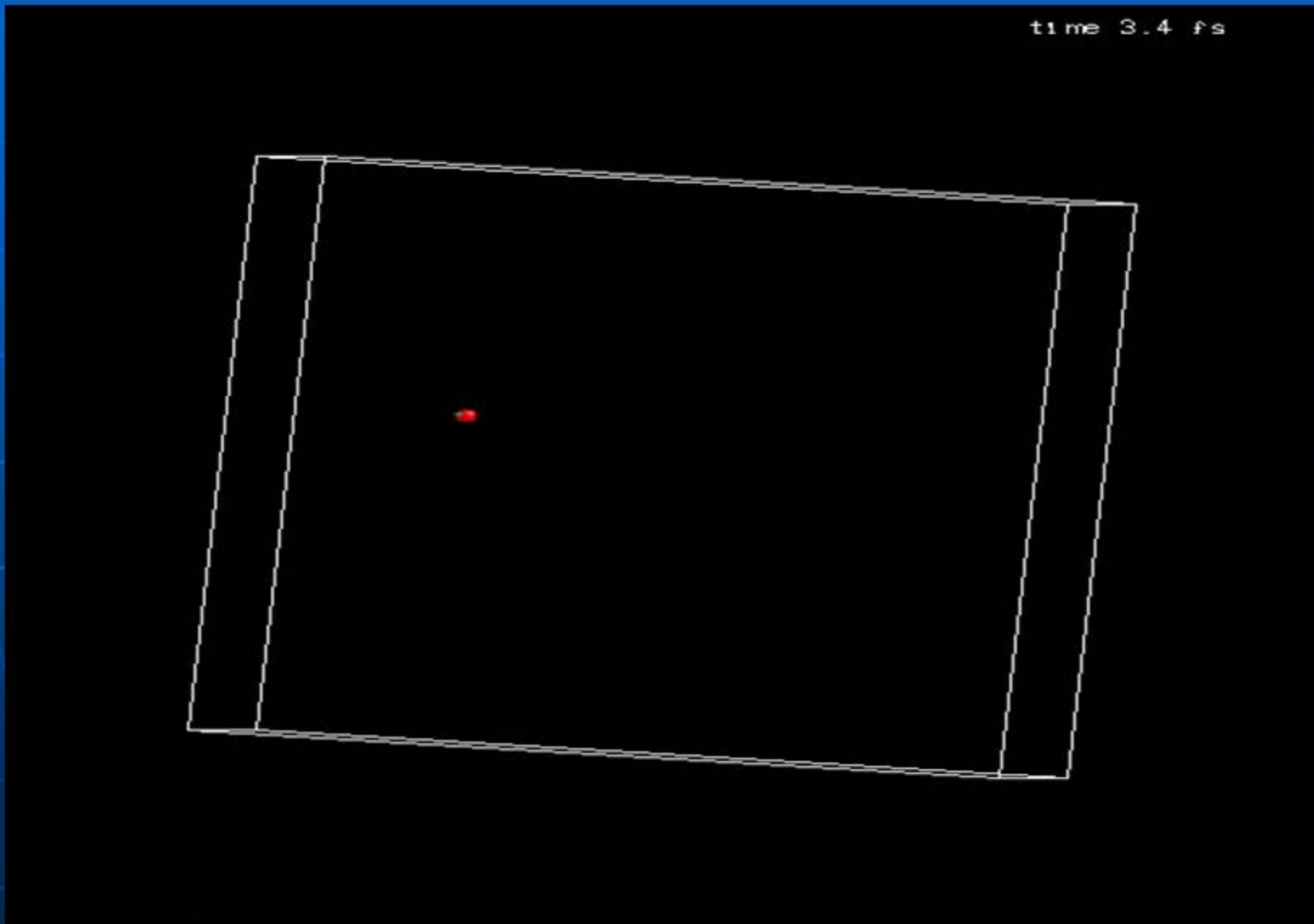
Multiscale modeling scheme

- primary radiation damage formation: molecular dynamic and kinetics Monte Carlo
- *ab initio* (VASP), according for H and He defects in materials, influence interatomic potentials on defect properties
- atomistic simulation of dislocation-defect interactions, molecular dynamics
- mesoscale (reaction rate theory) model of misrostructure evolution of irradiated materials

Methods for Calculations of Radiation Damage in Materials

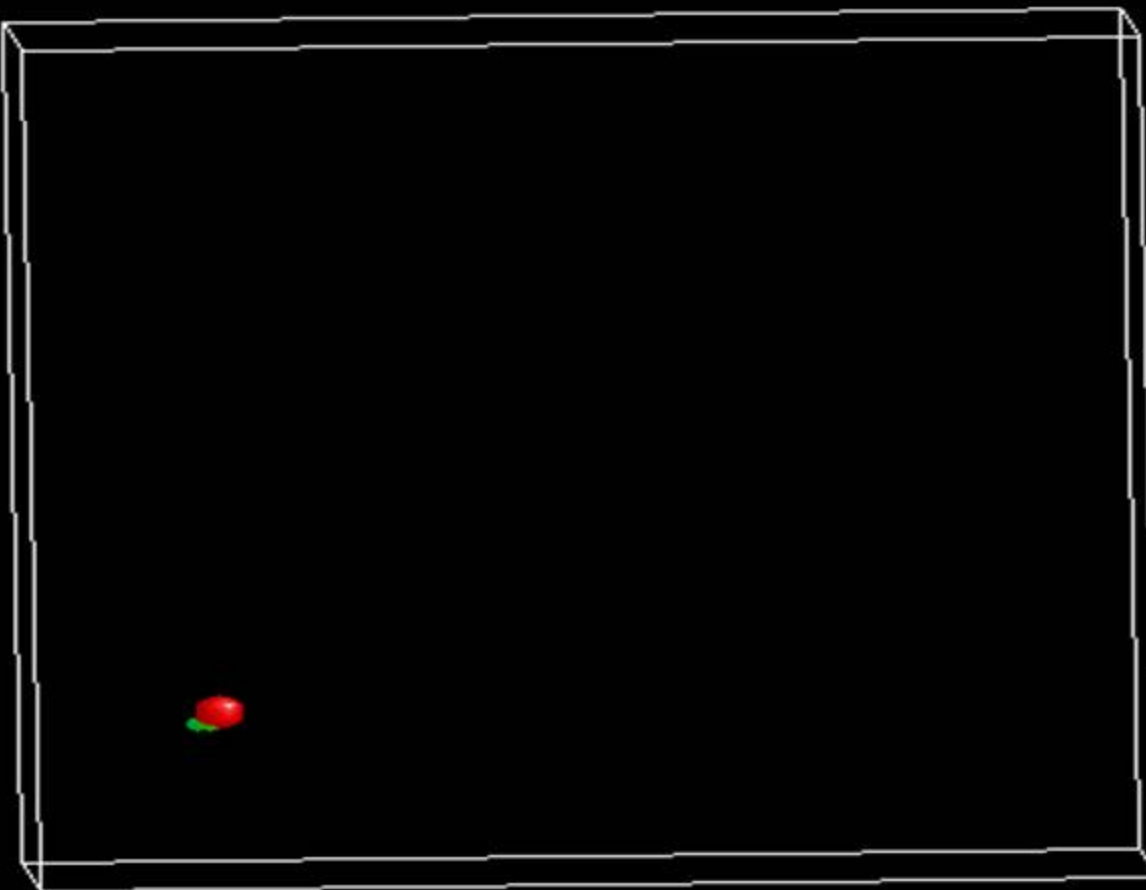


Cascade Formation in Al (PKA energy E = 10 KeV)



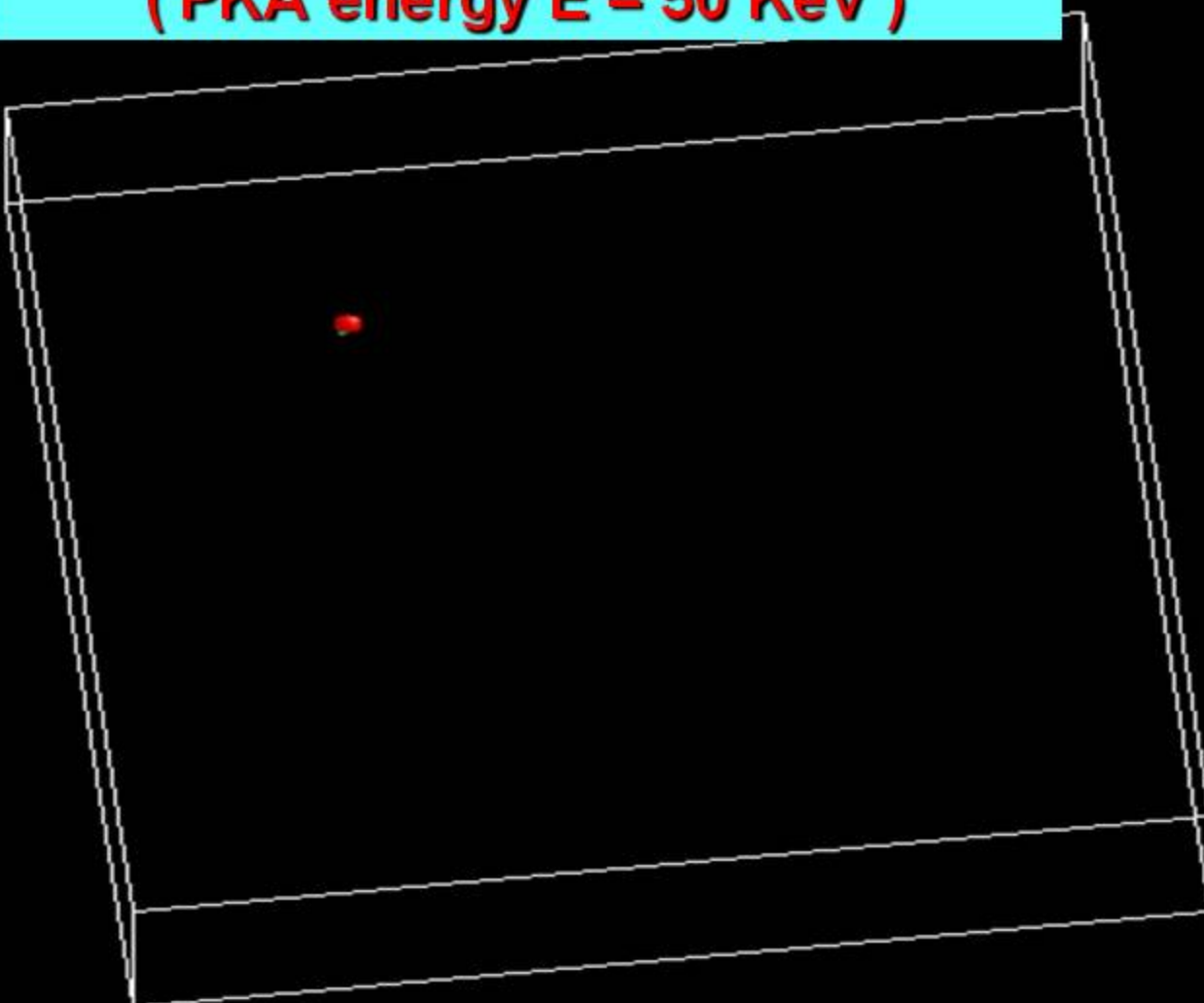
time 3.6 fs

Cascade Formation in Cu (PKA energy E = 10 KeV)



time 1.6 fs

Cascade Formation in Ni (PKA energy E = 50 KeV)

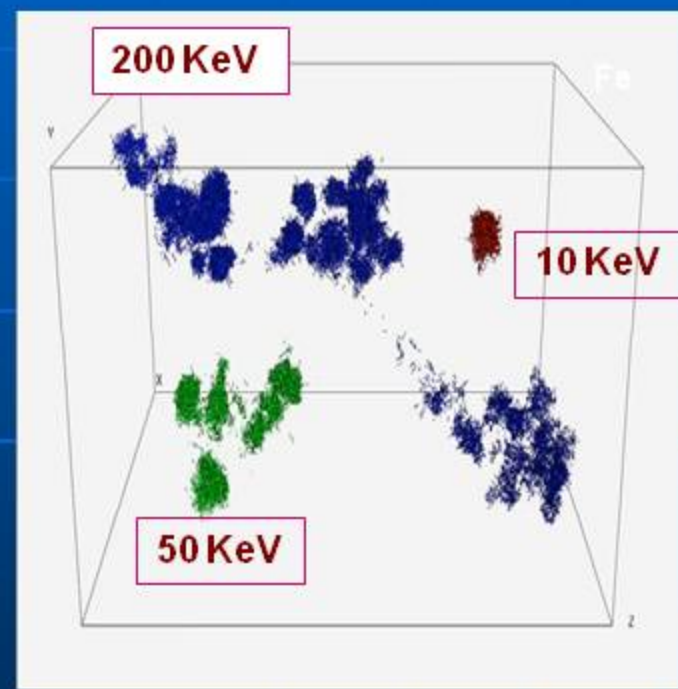
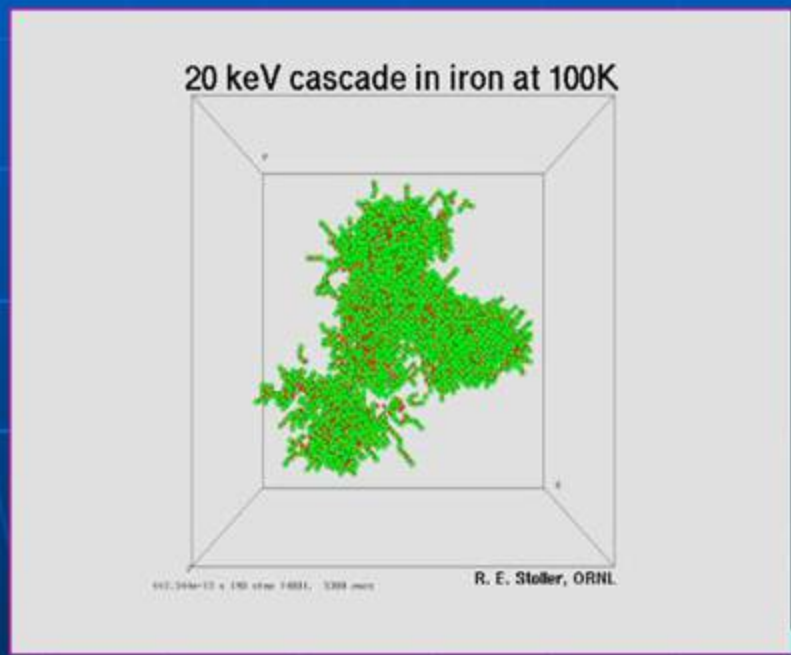


Data base for cascade formation in Fe at 100 K

MD Cascade Energy (keV)	Corresponding neutron energy (MeV)	Number of Simulations	Typical simulation cell size (atoms)
0.1	0.003351	40	3,456
0.2	0.006818	32	6,750
0.5	0.01749	20	16k/54k
1.0	0.03578	12	54k
2.0	0.07342	10	54k
5.0	0.1911	9	128k
10.	0.3968	15	125k/250k
20.	0.8321	10	250k
50.	2.277	9	2.249M
100.	5.085	10	5.030M
200.	12.31	3	9.826M

Molecular Dynamics simulations have found the primary damage formation is similar for fission and fusion neutrons

- subcascade formation leads to asymptotic behavior at high energies
- agrees with experimental data at low energy

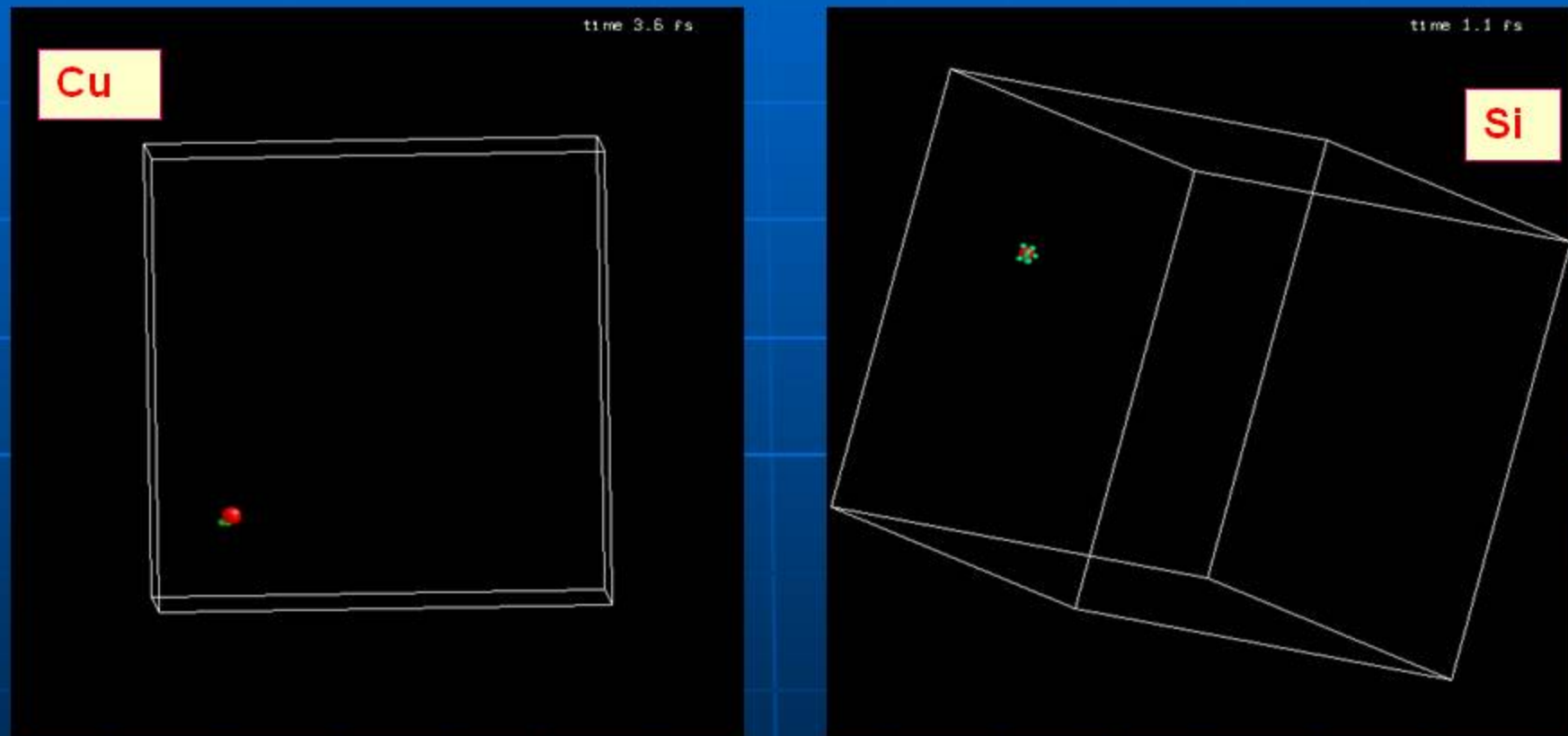


R.E. Stoller, 2004

Modeling of Cascade and Sub-cascade Formation in Fission and Fusion Structural Materials

- Introduction**
- Theoretical Model**
- Numerical Calculations of cascade and sub-cascade formation for different Fusion and Fission Neutron Facilities:
ITER, DEMO, IFMIF, HFIR.**
- Conclusions**

Comparison of cascade and sub-cascade formation in light and heavy materials.



K. Nordlund (1998)

Theoretical Model

- ↳ First idea was suggested by M. Kiritani :
Y. Satoh, S. Kojima, T. Yoshiie, M. Kiritani, J. Nucl. Mat., 179-181, (1991) 901.
Y. Satoh, T. Yoshiie, M. Kiritani, J. Nucl. Mat., 191-194, (1992), 1101.
- ↳ Some results from:
H.L. Heimisch, B.N. Singh , Philosophical Magazine A, vol. 67(1993) 407.
H.L. Heimisch, B.N. Singh , J.Nucl.Mat., 251 (1997) 77.
R.E. Stoller, Mat. Res. Soc. Symp. Proc. Vol. 373 (1995) 21.
R.E. Stoller, Proc. ICFRM-8, J.Nucl.Mat. 555 (1998) 10.
- ↳ Following development of theoretical model:
A.I. Ryazanov, E.V. Metelkin, Atomic Energy, v.83, No 3, (1997), 633.
- ↳ Binary elastic collision model is used for moving atoms with real interatomic potential.
- ↳ New criterion for sub-cascade formation is suggested.
- ↳ Sub-cascade formation cross - sections and generation rates of sub-cascades are calculated for different neutron energy spectra in fusion facilities.

Graphite

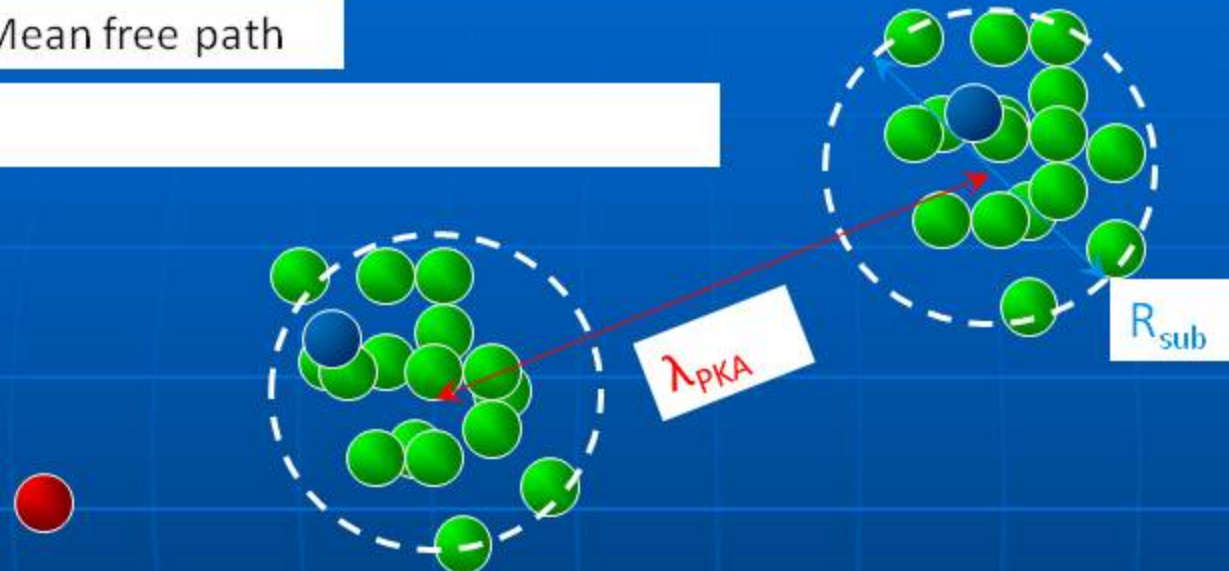
Copper

PKA

SKA

λ_{PKA} Mean free path

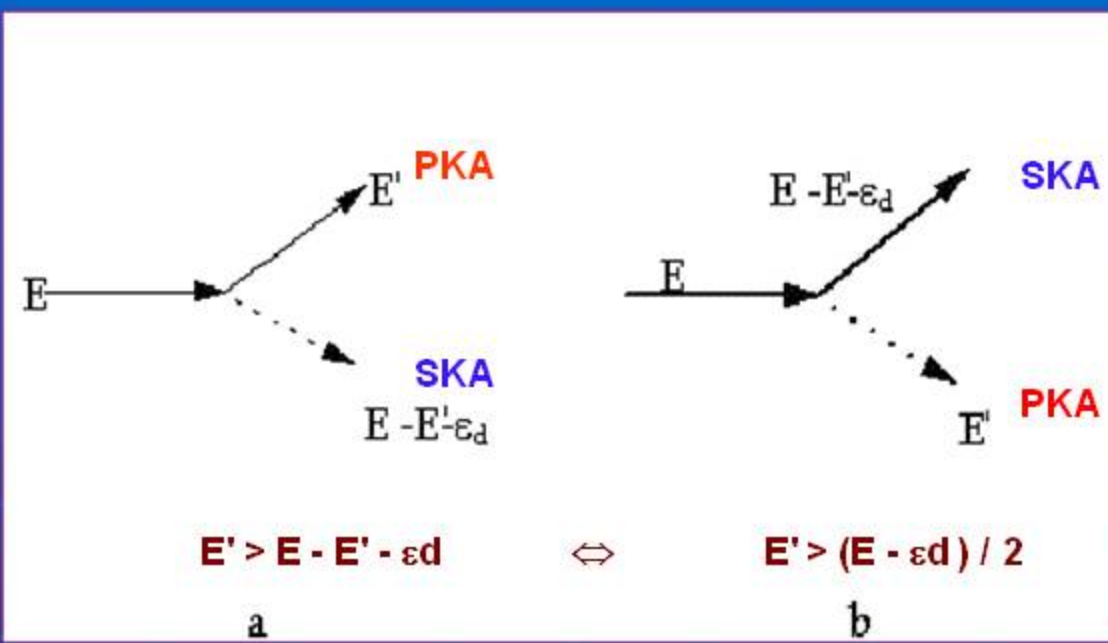
R_{sub}



Sub-cascade formation criterion:

$$\lambda_{\text{PKA}} \geq R_{\text{sub}}$$

Binary Collision Model



$\Sigma(E \rightarrow E')$ - the differential cross-section for incident atom with initial energy E to get after elastic collision energy E'

The cross-section $\Sigma(E, E_{sf})$ characterizing the collision with transfer energy higher than E_{sf}

$$\Sigma(E, E_{sf}) = \int_{E_{sf}}^{(E - \varepsilon_d)/2} dT [\Sigma(E \rightarrow E' - T - \varepsilon_d) + \Sigma(E \rightarrow T)] = \int_{E_{sf}}^{(E - \varepsilon_d)/2} dT P(E, T) \Sigma(E)$$

$\lambda_{PKA}(E)$ - the distance between two collisions

$$\lambda_{PKA}(E) = \frac{1}{N_a \Sigma(E, E_{sf})}$$

$R_{sub}(E, E_{sf})$ – the average size of damage zone produced by SKA

$$R_{sub}(E, E_{sf}) = \int_{E_{sf}}^{(E-E_{sf})/2} P(E, T) R(T) dT$$

$P(E, T)$ the probability density for SKA with initial energy E to have a kinetic energy T after collision

$R(T)$ the displacement depth of SKA with an initial kinetic energy T

$$R(T) = \int_0^T \frac{dT}{(dT/dx)_{tot}}$$

where $(dT/dx)_{tot} = (dT/dx)_n + (dT/dx)_e$ - the total stopping power including the elastic stopping power $(dT/dx)_n$ and inelastic (electronic losses) stopping power $(dT/dx)_e$

$$\lambda_{PKA} \geq R_{sub}$$

Threshold Energy for Sub-cascade Formation

	Cu	Ag	Au
Suggested Model	20 KeV	62 KeV	210 KeV
Monte Carlo Method	26 KeV	48 KeV	172 KeV

$$E_{sf}(KeV) = 0,0056Z^{2.415}$$

A.I.Ryazanov, E.V.Metelkin,
Atomic Energy, v.83, No 3, 1997, 653.

Number of Sub-cascades as a Function of PKA Energy

$$N_{sc}(E) = 1 + \int_{2E_{sf}}^E \frac{N_a \Sigma_{sf}(T) dT}{\left(\frac{dT}{dx} \right)_{tot}}$$

$\Sigma_{sf}(T)$ is the energy cross section for sub-cascade formation,

N_a is the density of target atoms,

$$\left(\frac{dT}{dx} \right)_{tot} = \left(\frac{dT}{dx} \right)_n + \left(\frac{dT}{dx} \right)_e$$

$$\left(\frac{dT}{dx} \right)_n = \frac{N_a \epsilon}{T} \int_0^{T/\epsilon^2} \left(\frac{\pi a^2}{2t^{1/2}} \right) \frac{\lambda t^{1/2-m} dt}{(1 + (2\lambda t^{1-m})^q)^{1/q}}$$

$$\left(\frac{dT}{dx} \right)_e = N_a (S_L(T)^{-1} + S_{BB}(T)^{-1})^{-1}$$

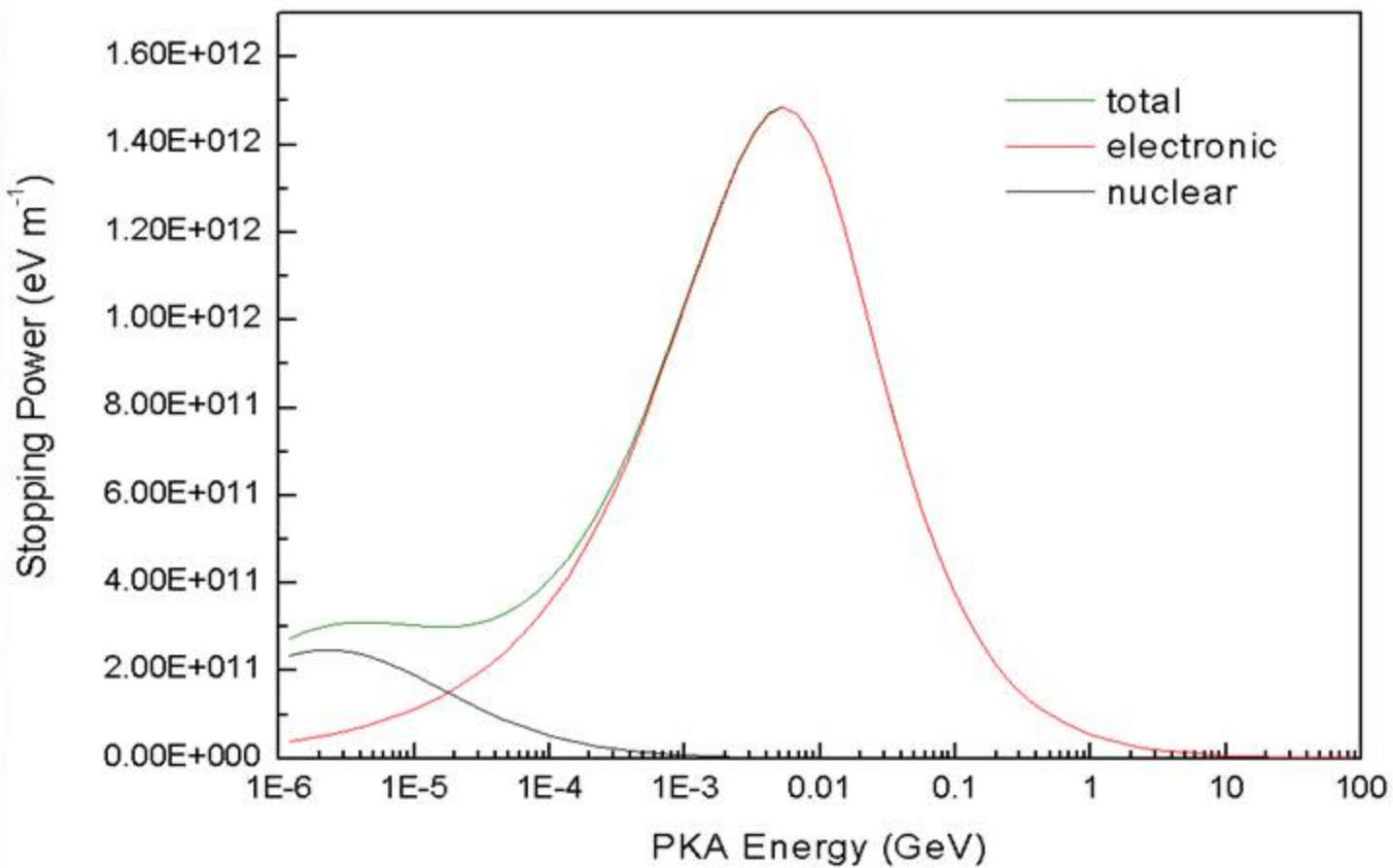
$$S_L(T) = k_L T^{1/2}$$

$$k_L = \frac{4 a_0 h \sqrt{2} Z_i^{7/6} Z_T}{(Z_i^{2/3} + Z_T^{2/3})^{3/2} \sqrt{M_i}}$$

$$S_{BB}(T) = \frac{8\pi Z^2 e^4}{I \epsilon_b} \ln \left(\epsilon_b + 1 + \frac{5}{\epsilon_b} \right)$$

$$\epsilon_b = \frac{4 T m_e}{Z_T I \cdot M_i}$$

Total Energy Loss for Moving Atoms in Graphite



Calculations of Cross Sections of Sub-cascade Formation in Different Materials

$$\Sigma_{sf}(E_n) = \int_{E_{sf}}^{E_{max}} \sigma_{el}(E_n, T) N_{sc}(T) dT$$

$\Sigma_{sf}(E_n)$

- Cross section of sub-cascade formation as a function of neutron energy E_n

$\sigma_{el}(E_n, T)$

- Differential elastic cross section for scattering of fast neutron with energy E_n on atom with the energy transfer T to atom

$N_{sc}(T)$

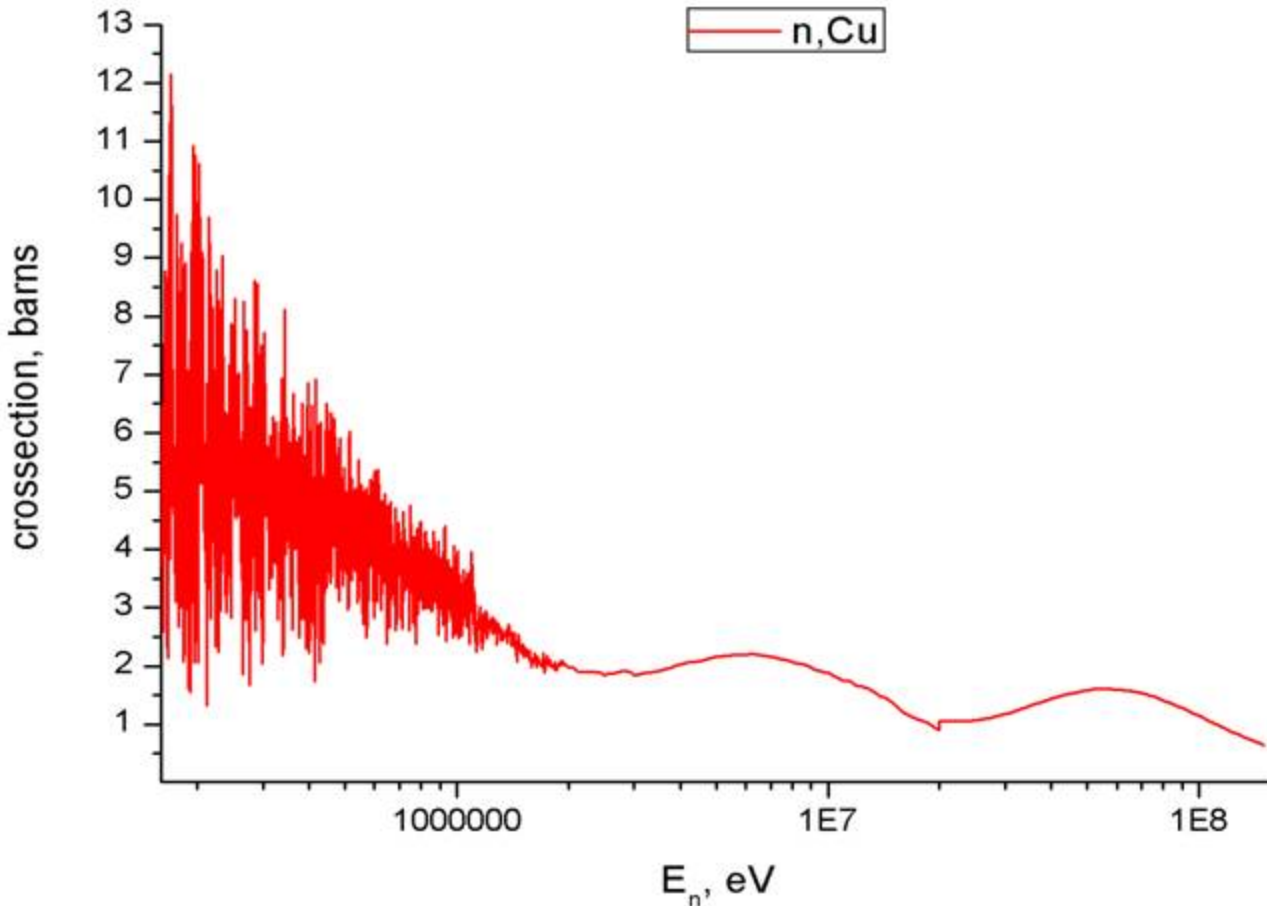
- Number of sub-cascades produced by PKA with energy T

E_{sf}

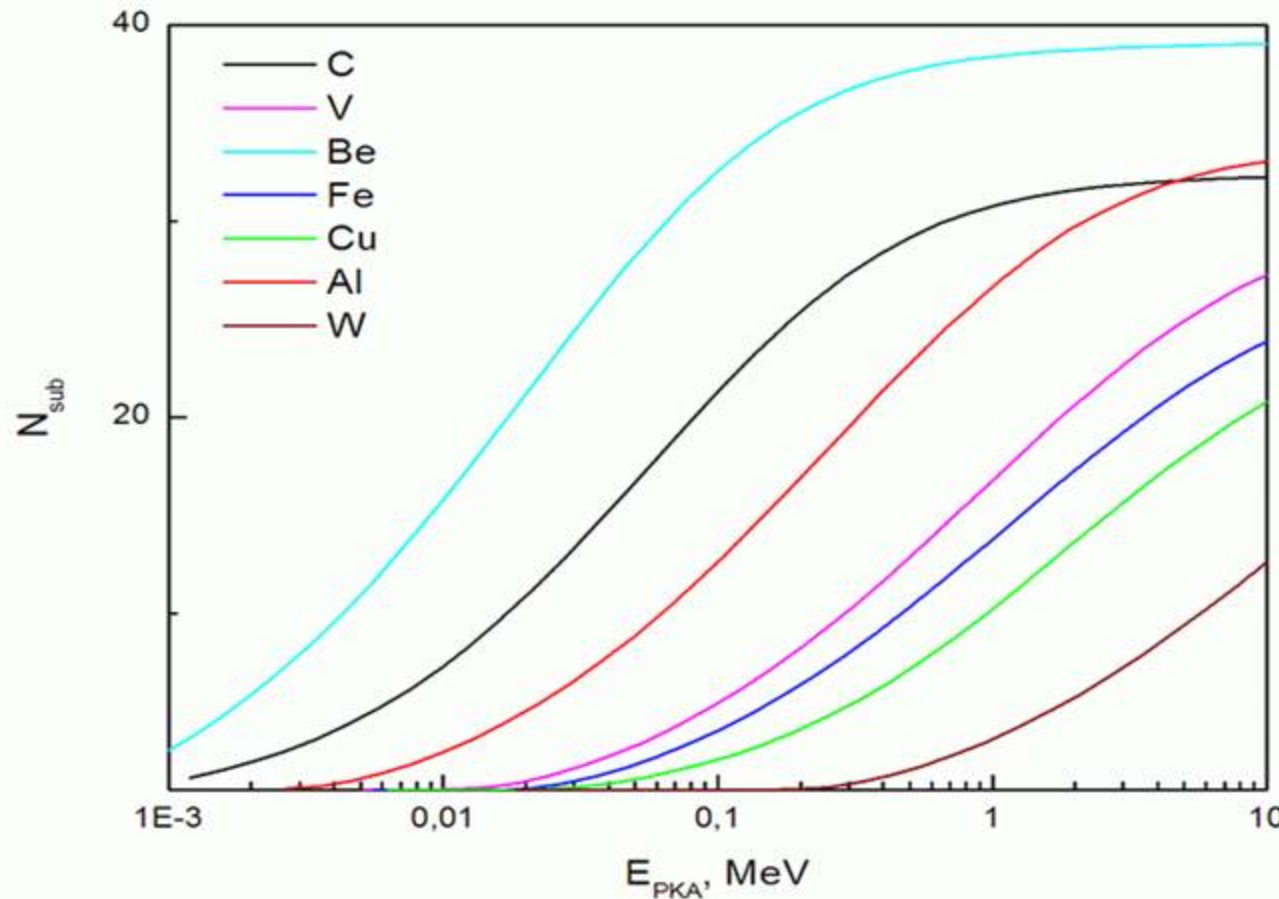
- Sub-cascade formation energy

$$E_{max} = E_n \frac{4m_n M_{PKA}}{(m_n + M_{PKA})^2}$$

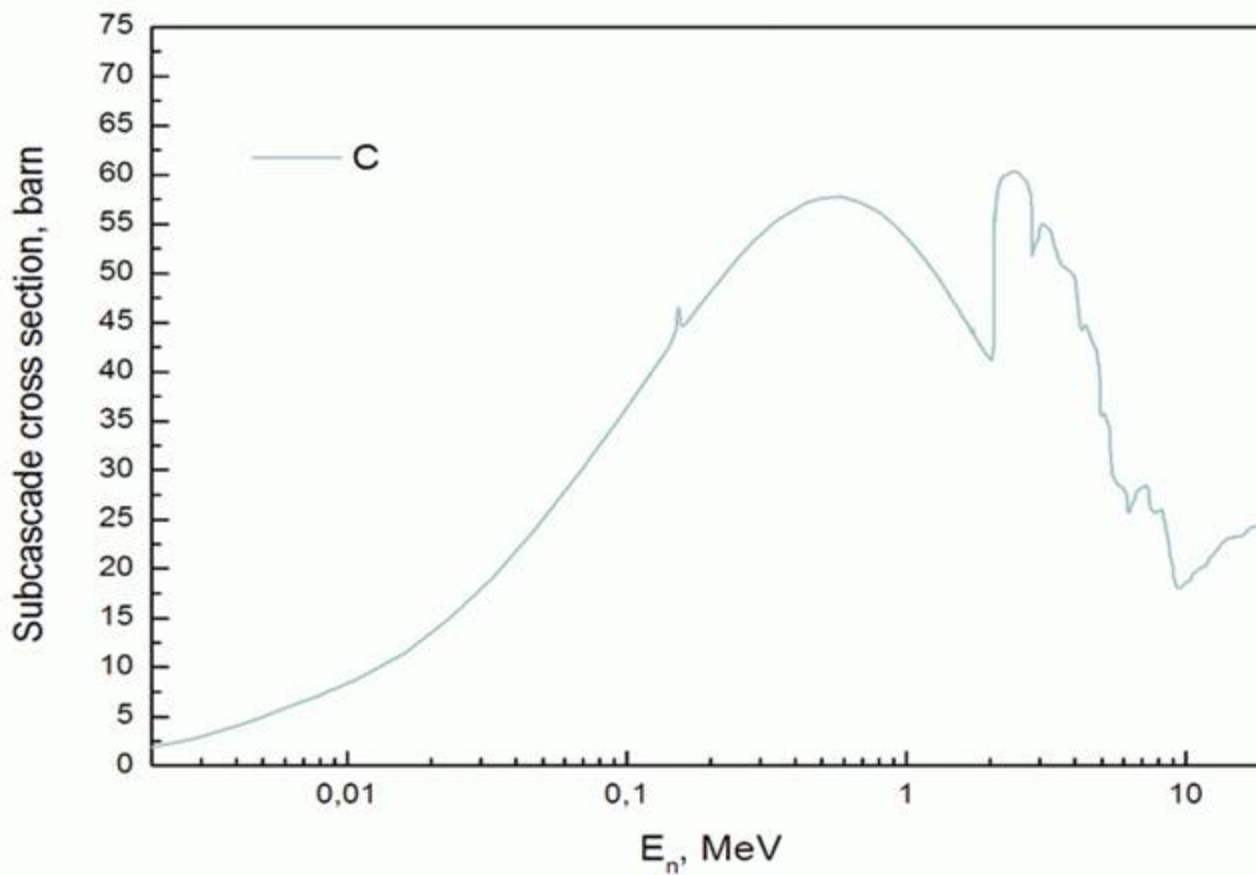
Cross section of elastic interaction of fast neutrons with Cu Atoms (from ENDF-B IV)



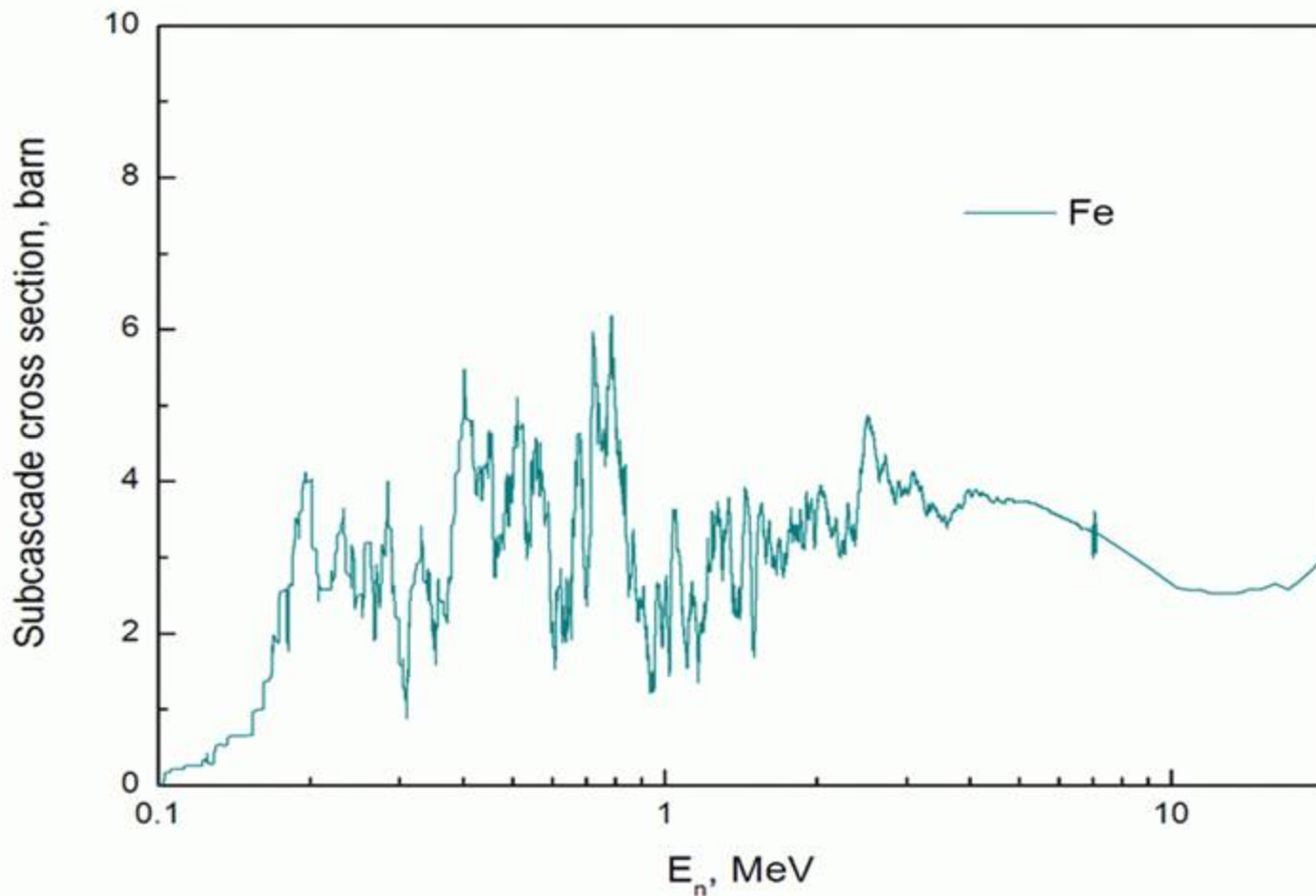
Number of Sub-cascades as a Function of PKA Energy



Cross Section of Sub-cascade Formation in C as a Function of Neutron Energy



Cross Section of Sub-cascade Formation in Fe as a Function of Neutron Energy



Calculations of Sub-cascade Generation Rates in different Materials under Neutron Irradiation

$$G_{sf}(E_n) = \int_{E_{sf}}^{E_n} \Phi(E'_n) \Sigma_{sf}(E'_n) dE'_n$$

$G_{sf}(E_n)$

- Generation rate of sub-cascade formation as a function of neutron energy E_n

$\Sigma_{sf}(E'_n)$

- Cross section of sub-cascade formation as a function of neutron energy E_n

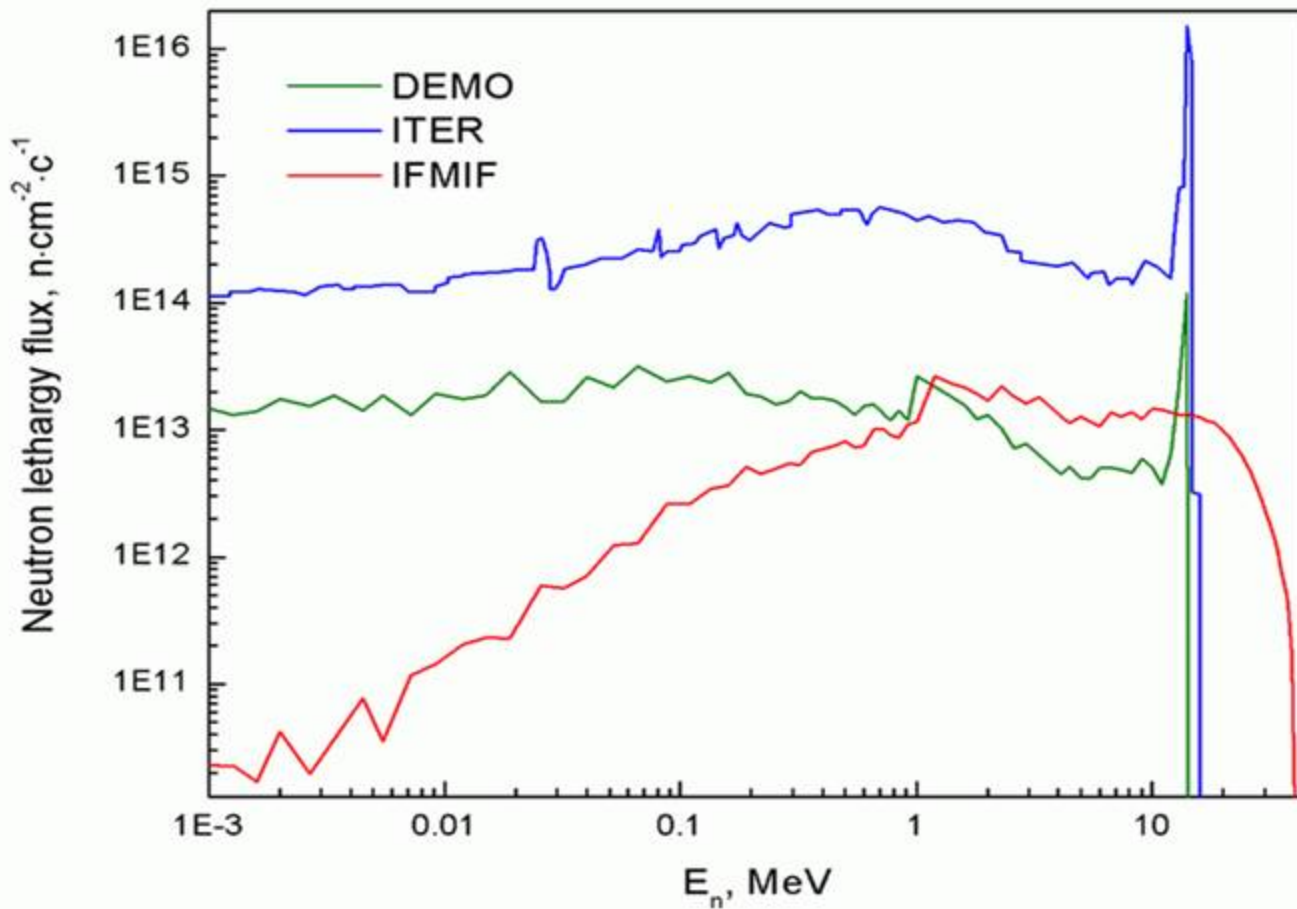
$\Phi(E'_n)$

- Energy flux of fast neutrons in differential fusion facilities

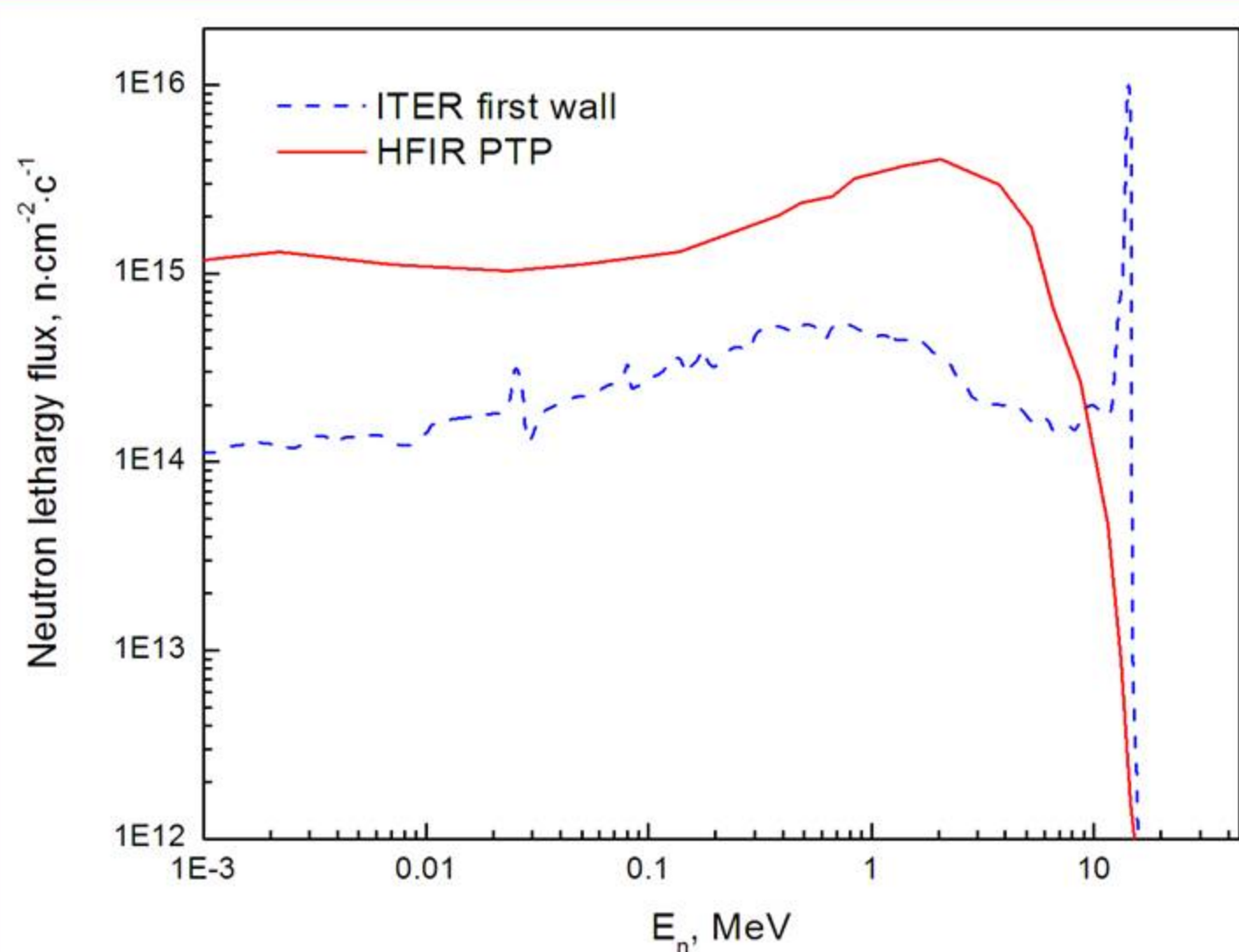
E_{sf}

- Sub-cascade formation energy

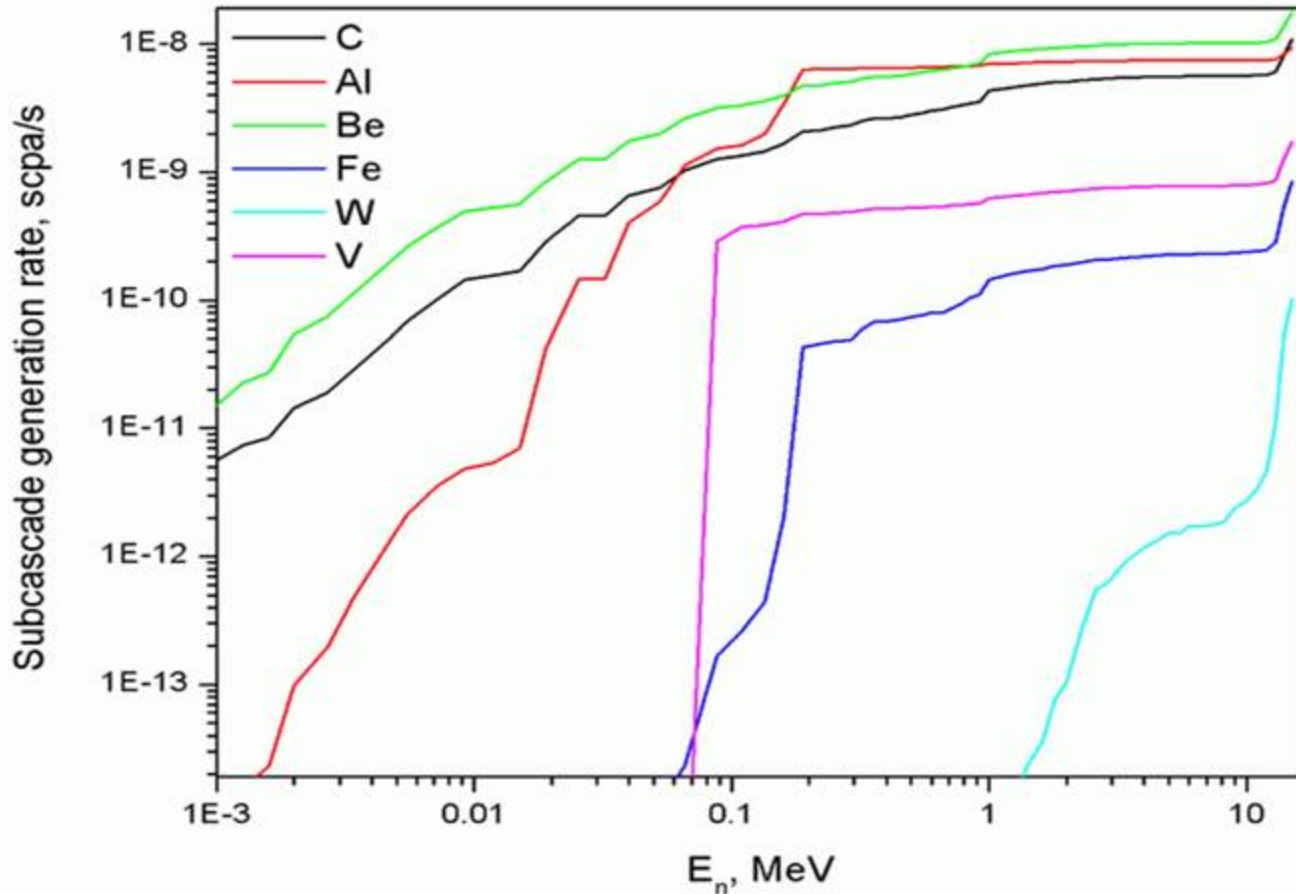
Neutron Energy Fluxes for different Fast Neutron Facilities



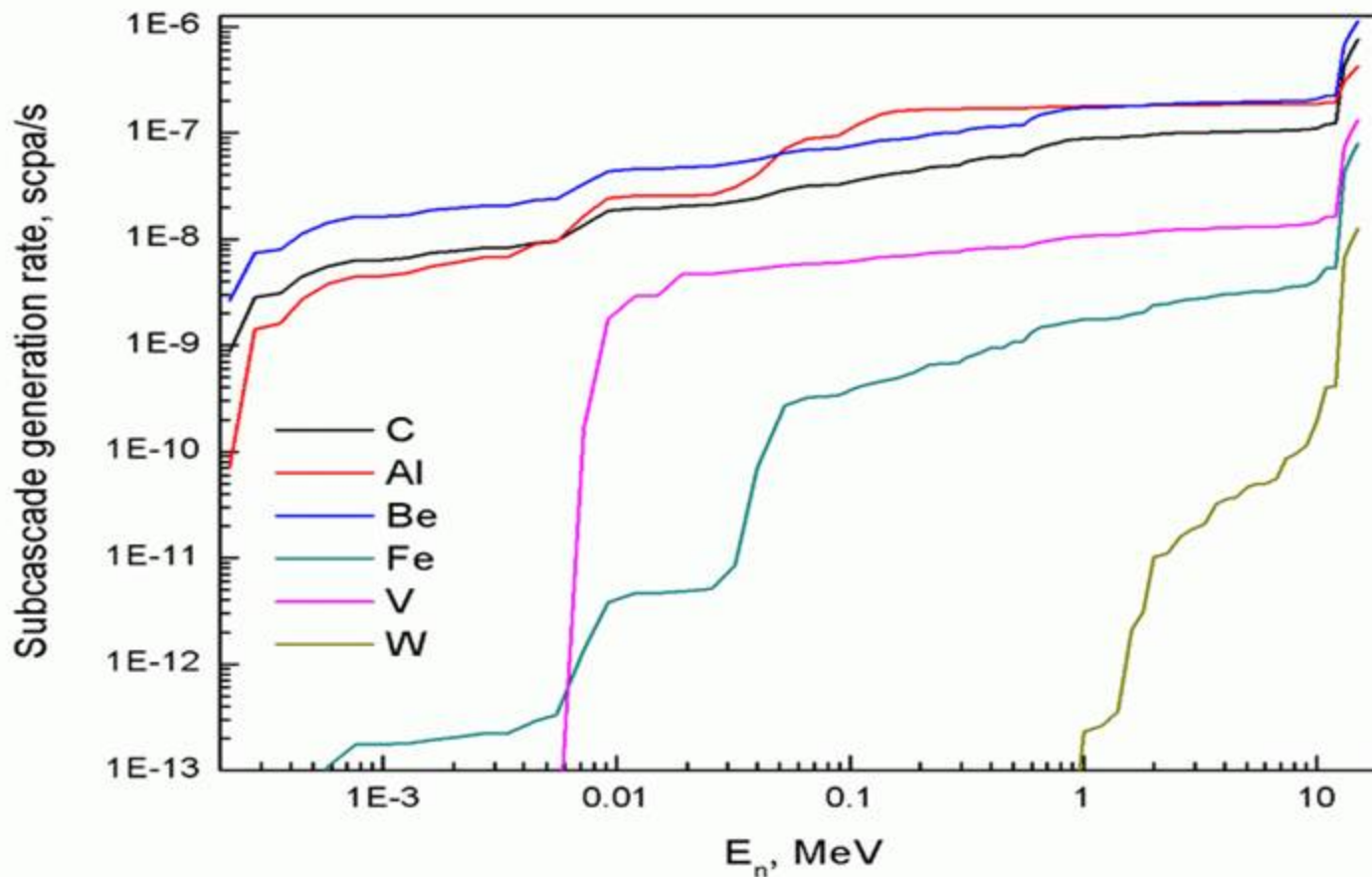
Neutron Energy Fluxes for different Fast Neutron Facilities (HRIR, ITER)



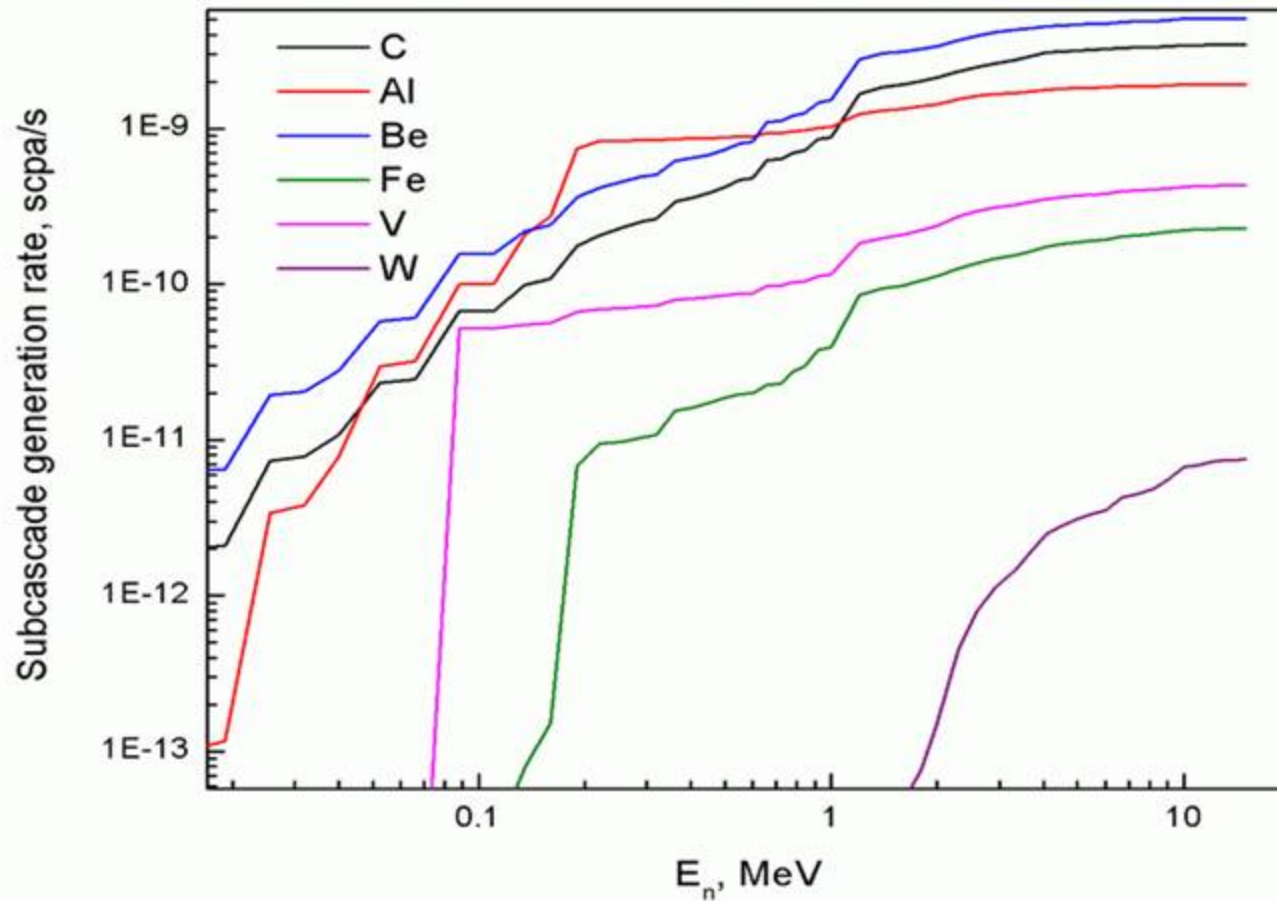
Sub-cascade Generation Rate in different Materials under Neutron Irradiation in DEMO



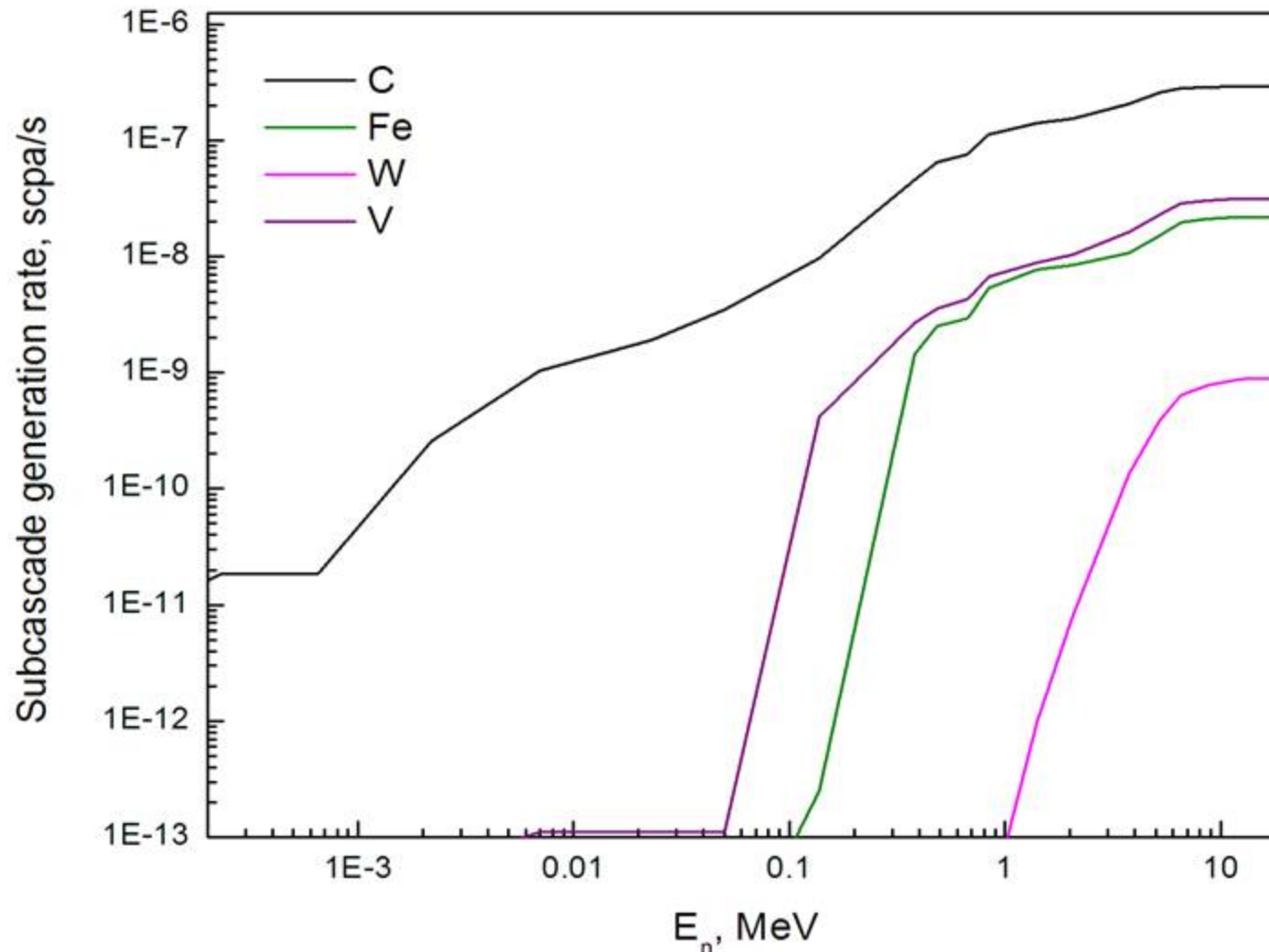
Sub-cascade Generation Rate in different Materials under Neutron Irradiation in ITER



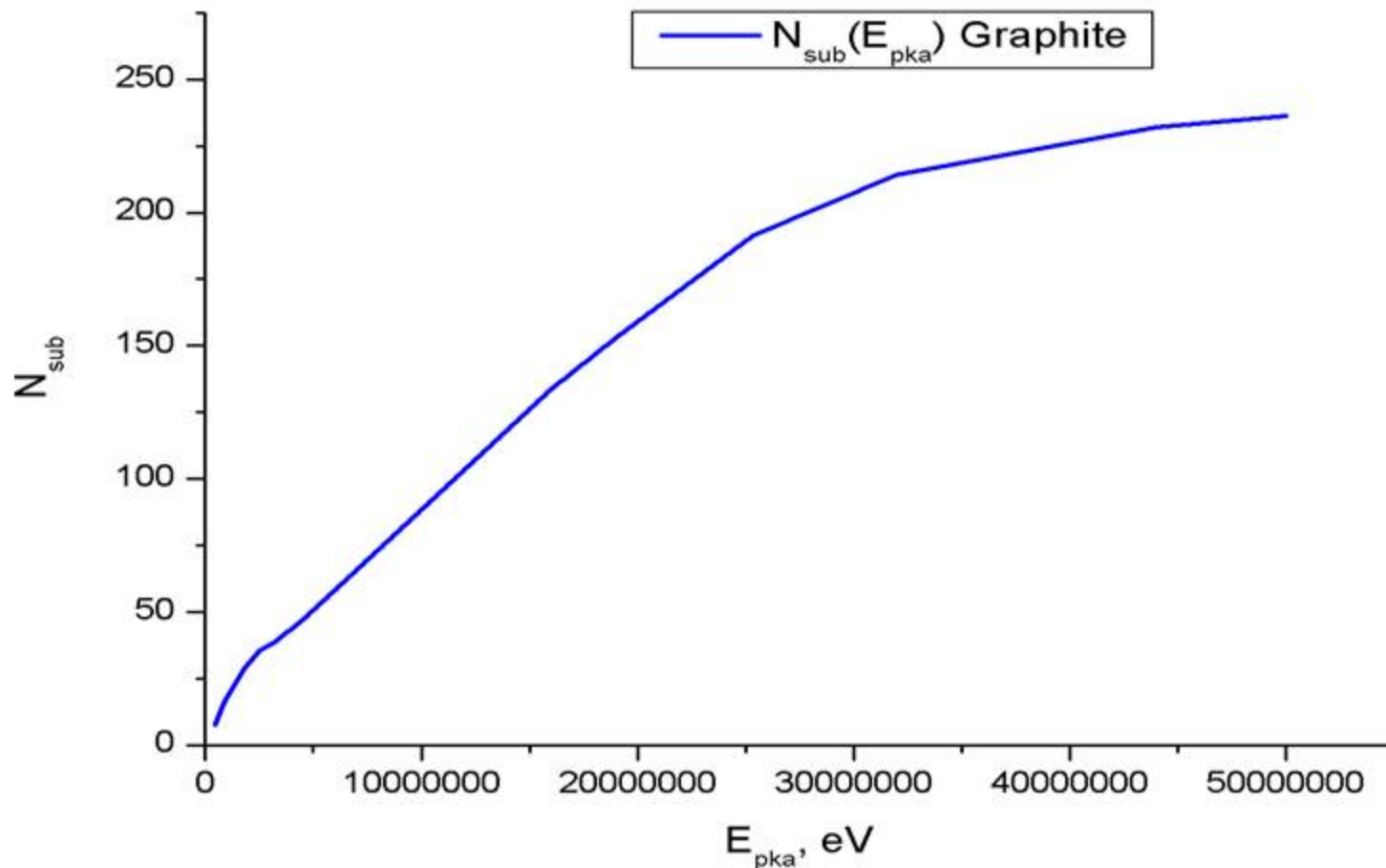
Sub-cascade Generation Rate in different Materials under Neutron Irradiation in IFMIF



Sub-cascade Generation Rate in different Materials under Neutron Irradiation in HFIR



Number of Sub-cascades in C as a Function of PKA Energy



Radiation Resistance of Graphite Materials

Graphite materials in Tokamaks and Fusion Reactor:

- **Limiter and/or protection plate for the inner wall**
Exposition to:

- **Vacuum**
- **Intense heat load**
- **Edge plasma**
- **Fast neutrons**

Important behavior:

- **Thermal shock resistance**
- **Thermo-mechanical properties**
- **Accumulation of Hydrogen and Helium in fusion reactor**
- **Accumulation of Radiation Damage**
- **Sputtering and particle emission**

Graphite Materials for Atomic Reactors :

- **Reflectors and stopping system of neutrons**

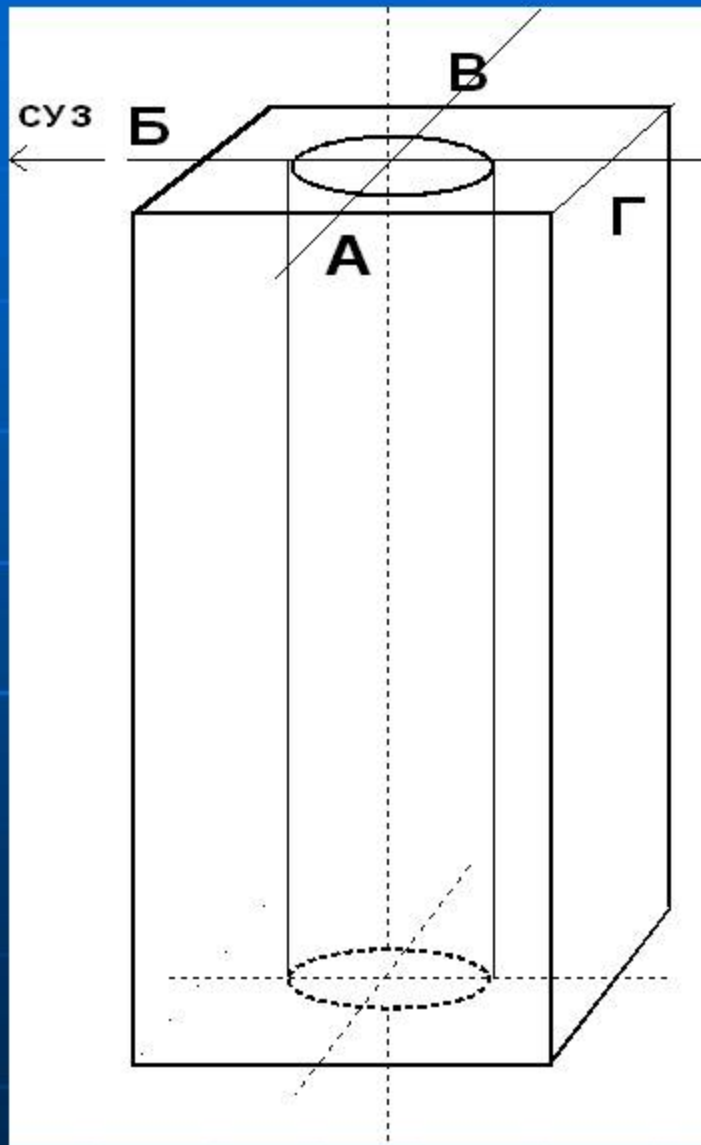
Exposition to:

- **Temperature: $T = 300-750 \text{ C}$**
- **Thermal and Fast neutrons**

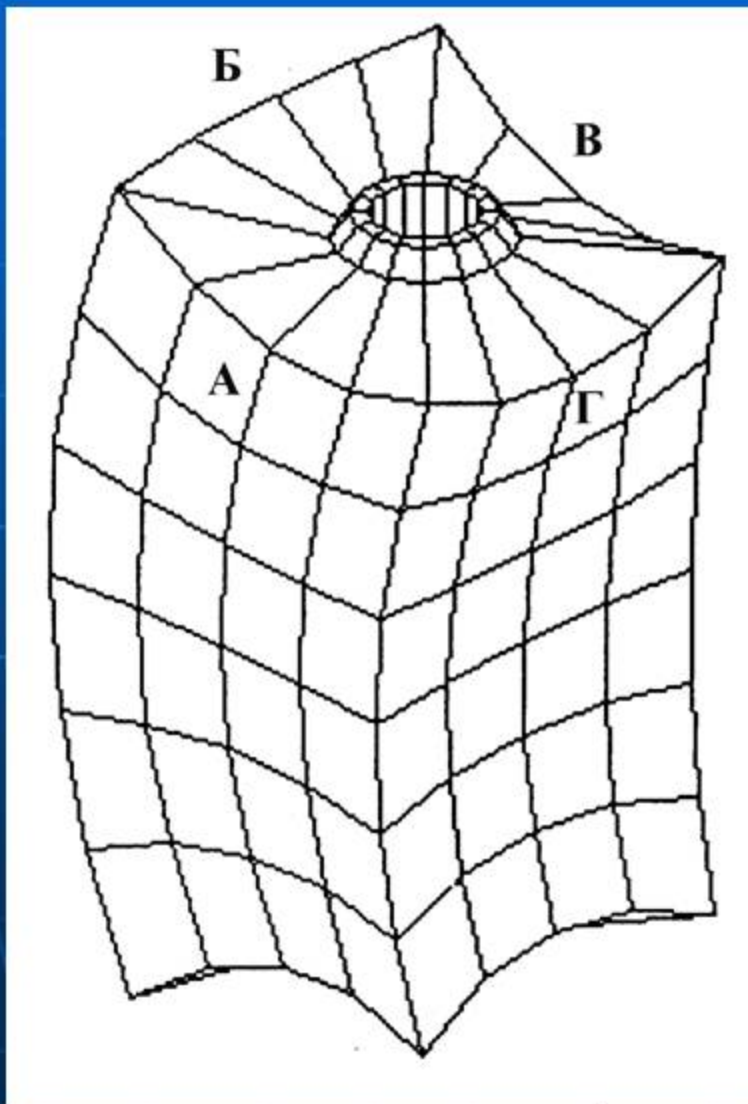
Important behavior:

- **Radiation swelling**
- **Degradation of thermo-mechanical properties**
- **Cracking and fracture**

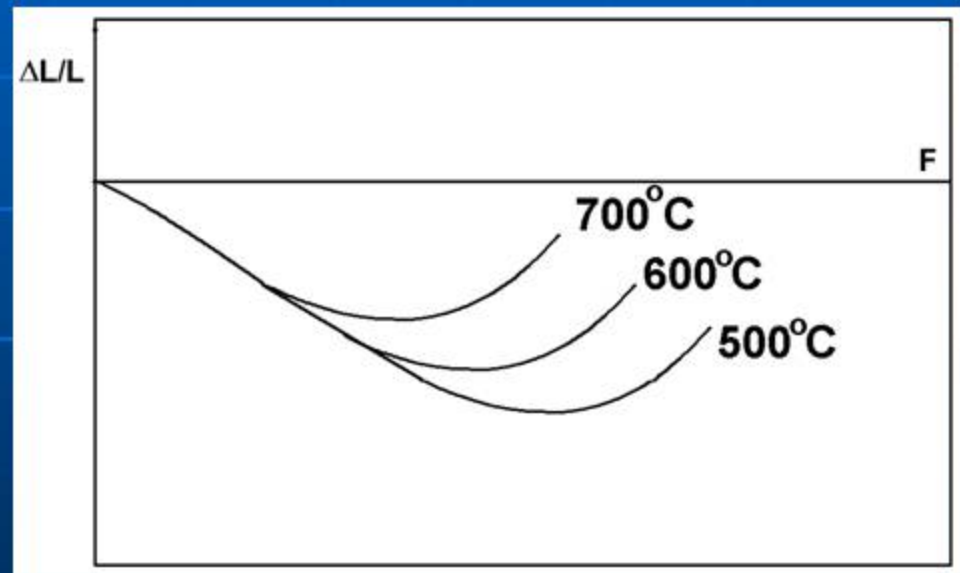
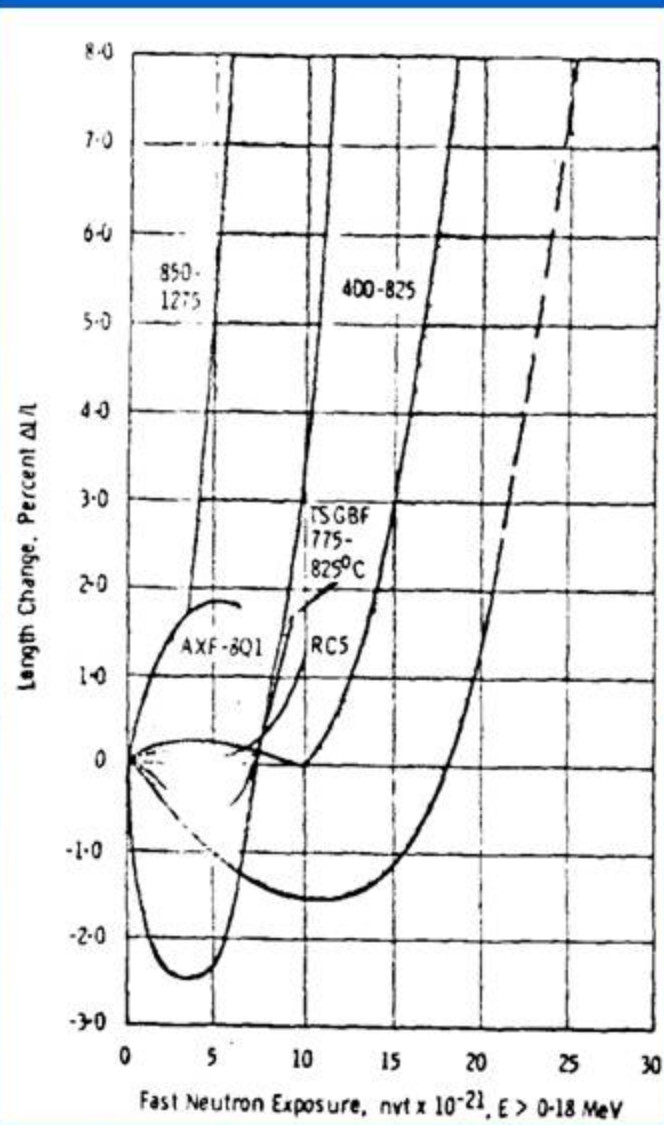
Graphite Sheave for Atomic Station



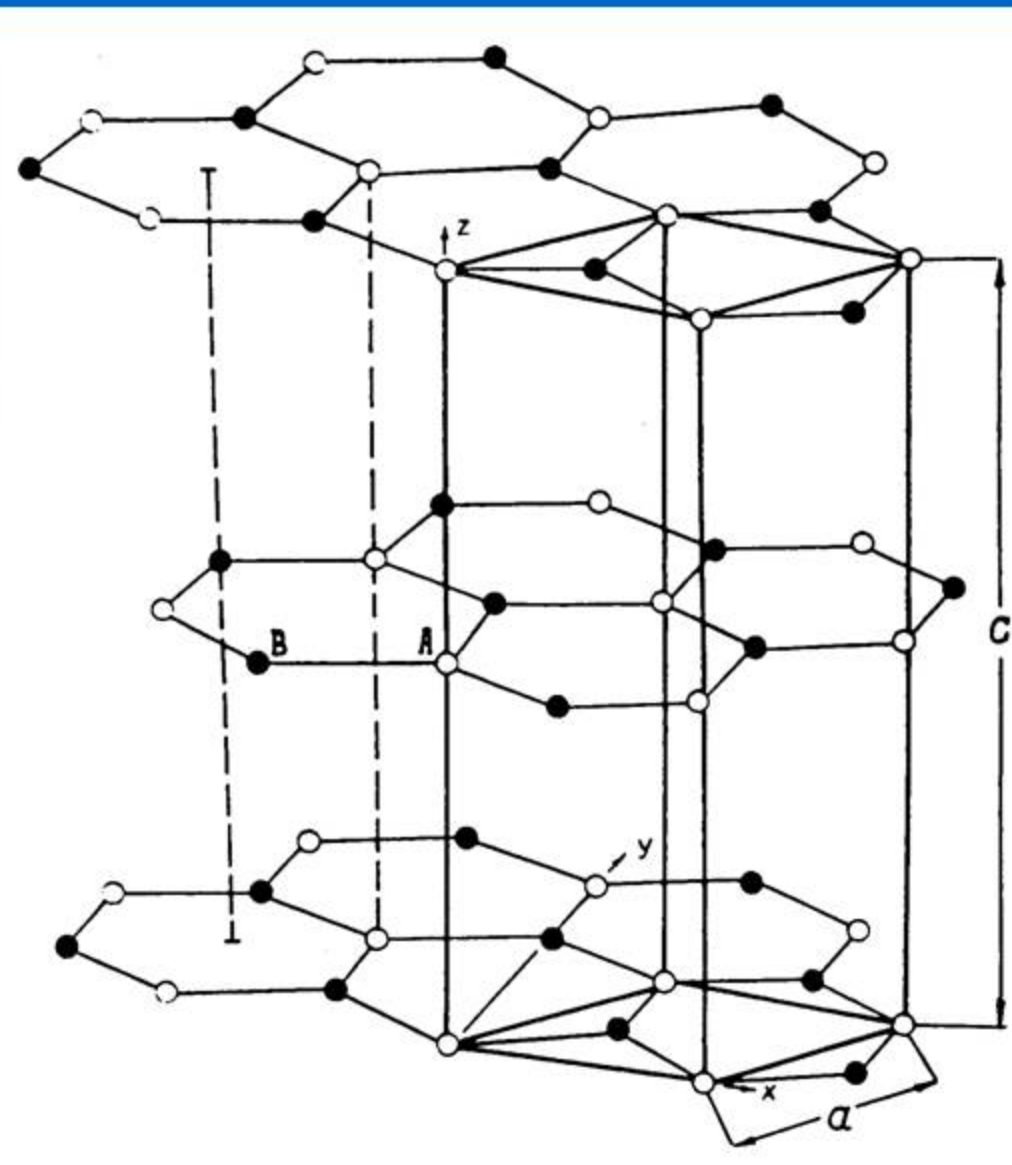
Graphite Sheave after Irradiation in Atomic Station



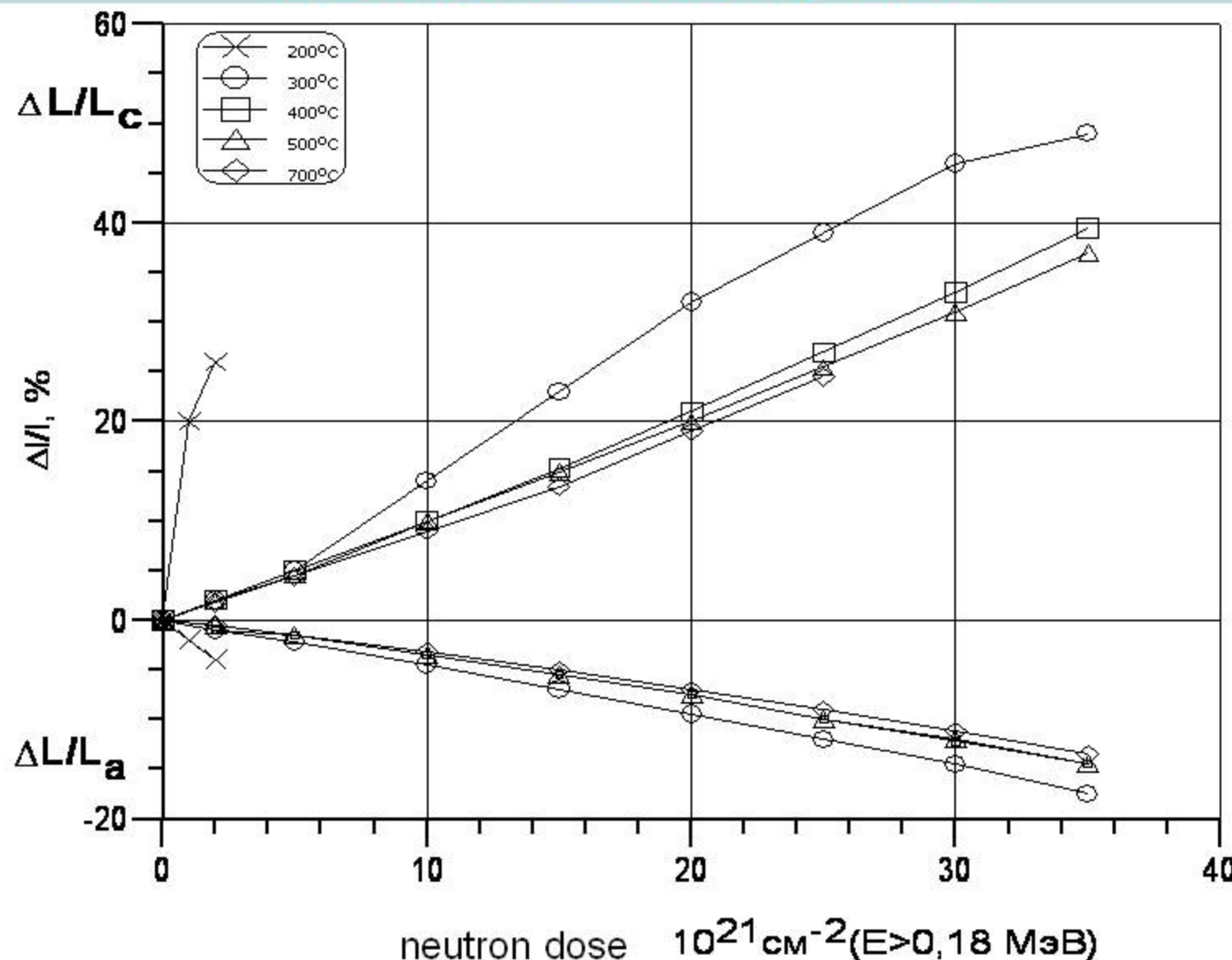
Radiation Shrinkage and Swelling of Graphite



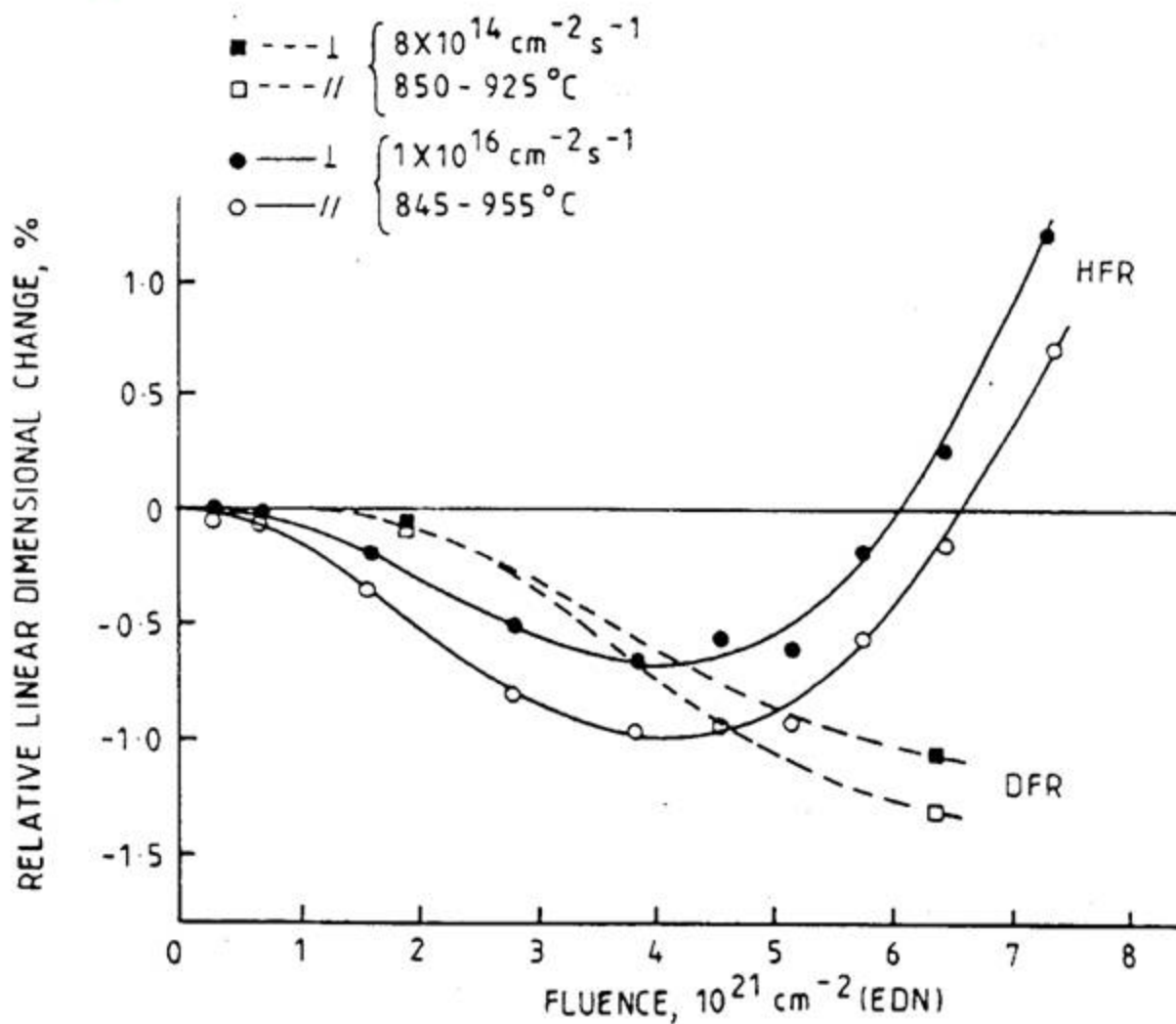
Graphite Elementary Cell



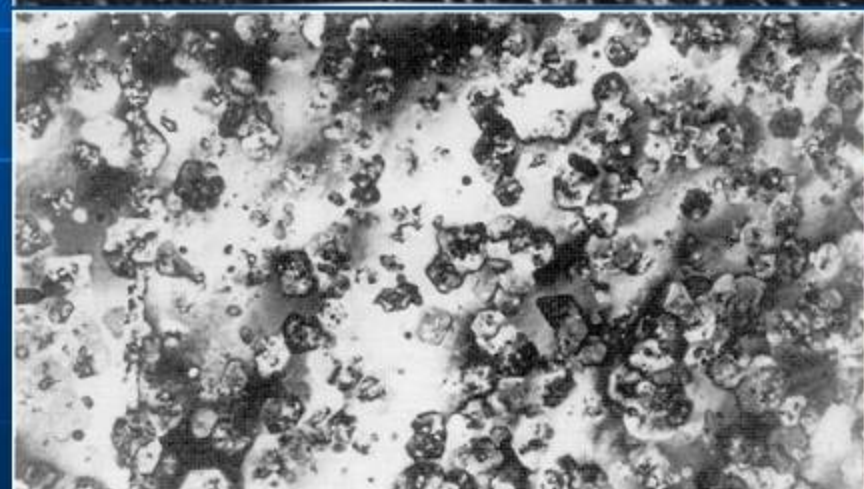
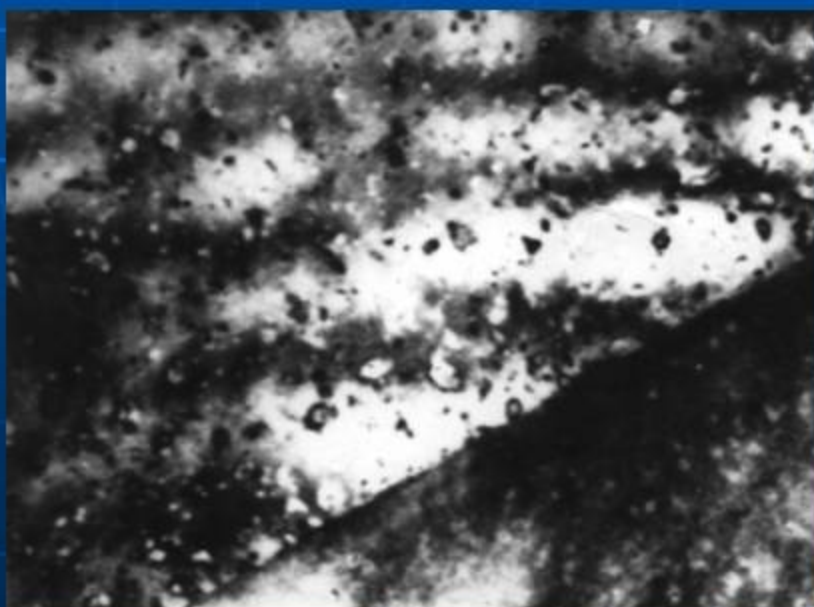
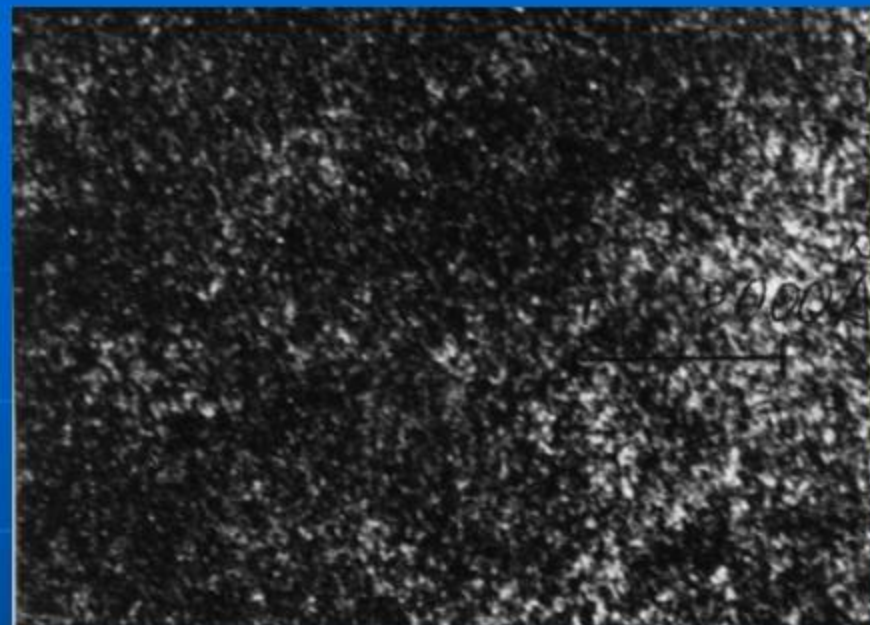
Cell Size Change of Irradiated Pyrographite in Dependence on Irradiation Dose and Temperature



Dose dependence of radiation swelling of graphite under neutron irradiation



Radiation Damage in Graphite



**B.Gurovich, P.Platonov, V.Schtombah,
RRC KI**

Development of Theoretical Models for the Calculations of Radiation Swelling in Carbon and SiC Materials.

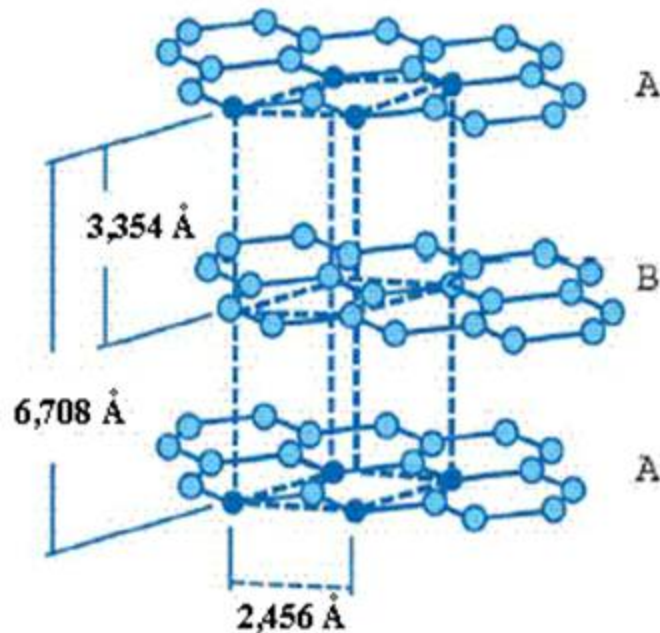
Materials:

- **SiC**
- **Graphite**

Physical Processes:

- **Generation of Point Defects**
- **Recombination of Point Defects**
- **Nucleation of Dislocation Loop**
- **Growth of Dislocation Loops**
- **Radiation Swelling**

Graphite - two diametrical anisotropic diffusivity



Crystallattice of graphite

Current of point defects on dislocation loop:

$$J_L = -2\pi b Z_L D_m C_m$$

Current of point defects on spherical void:

$$J_V = -4\pi R_V Z_V D_m C_m$$

Current of point defects on disk void:

$$J_S = -2\pi d Z_S D_m C_m$$

Radiation swelling of graphite in a and c -directions due to point defects:

$$\frac{\Delta a}{a} = -0.14(C_i + C_v), \frac{\Delta c}{c} = 3C_i + 0.2C_v$$

Radiation swelling of graphite in a and c-directions due to interstitial dislocation loops:

$$\frac{\Delta a}{a} = -0.014N_L V_L, \frac{\Delta c}{c} = 1.273N_L V_L$$

The total radiation swelling of graphite due to point defects, interstitial dislocation loops and vacancy voids:

$$S = 2 \frac{\Delta a}{a} + \frac{\Delta c}{c} = 2,72C_i - 0,08C_v + 1,242N_L V_L + \Delta \rho_V$$

The kinetics of point defects is described by the following equations:

$$\frac{dC_i}{dt} = G - \alpha D_i C_i C_v - (2\pi Z_L^i b N_L + 4\pi Z_V^i R_V N_V + 2\pi Z_S^i d N_S) D_i C_i,$$

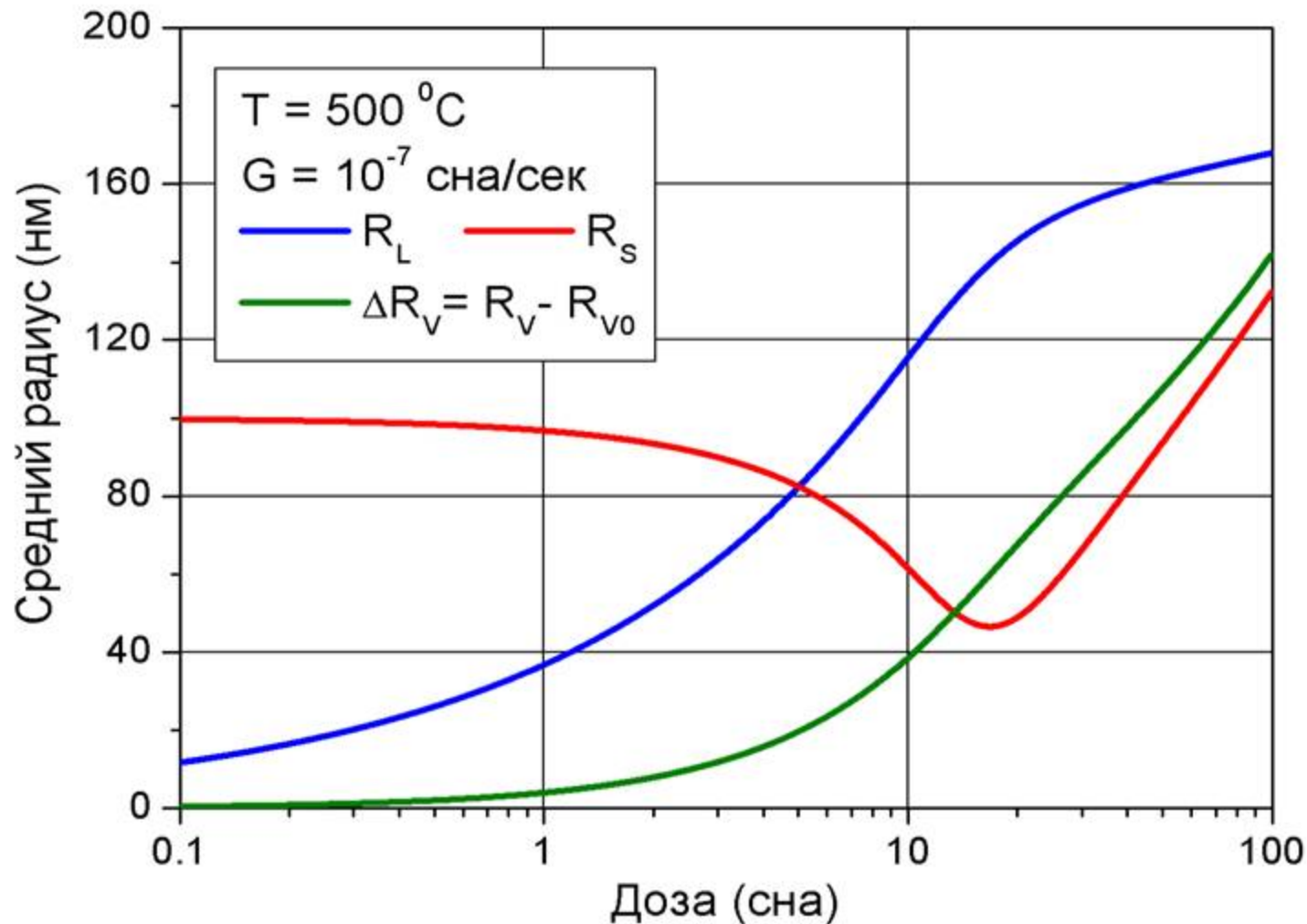
$$\frac{dC_v}{dt} = G - \alpha D_i C_i C_v - (2\pi Z_L^v b N_L + 4\pi Z_V^v R_V N_V + 2\pi Z_S^v d N_S) D_v C_v,$$

$$\frac{dR_L}{dt} = \frac{1}{R_L} (Z_L^i D_i C_i - Z_L^v D_v C_v),$$

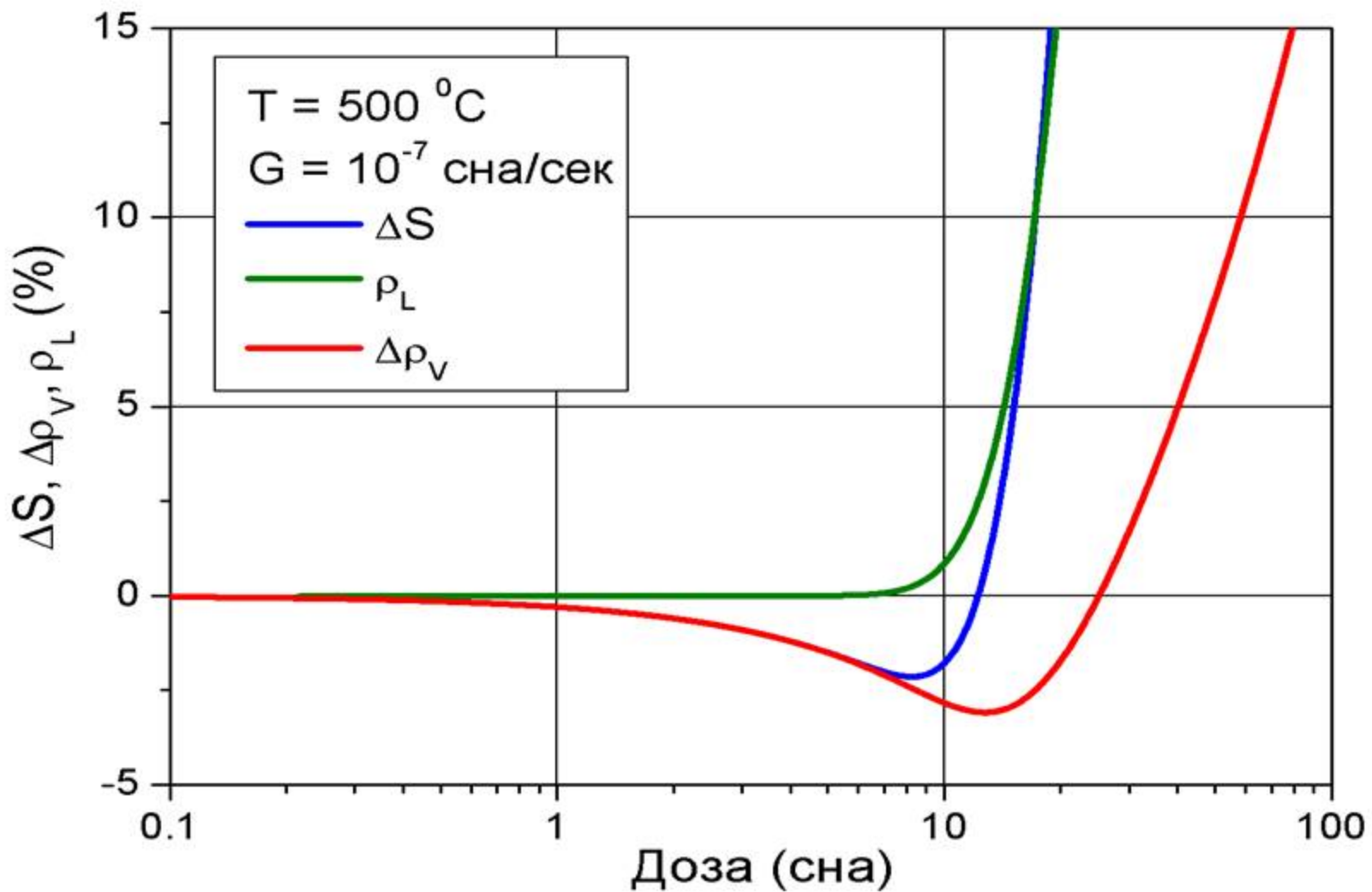
$$\frac{dR_V}{dt} = \frac{1}{R_V} (Z_V^v D_v C_v - Z_V^i D_i C_i),$$

$$\frac{dR_S}{dt} = \frac{3}{2R_S} (Z_S^v D_v C_v - Z_S^i D_i C_i),$$

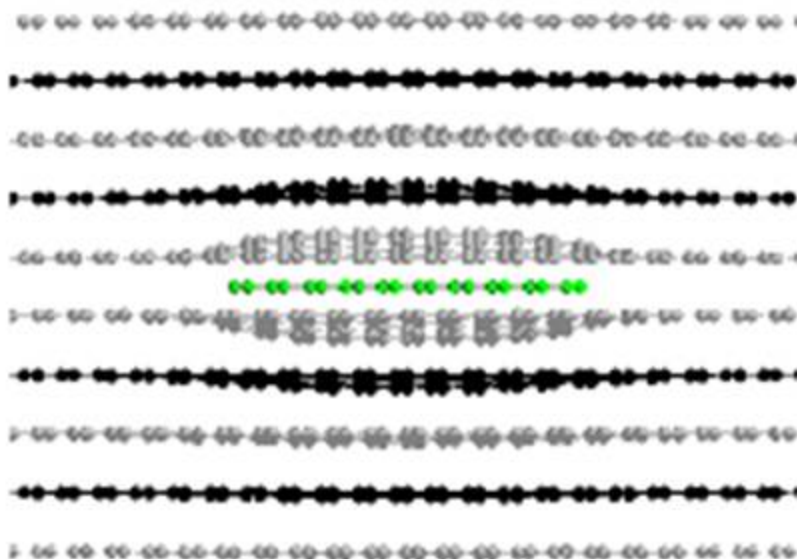
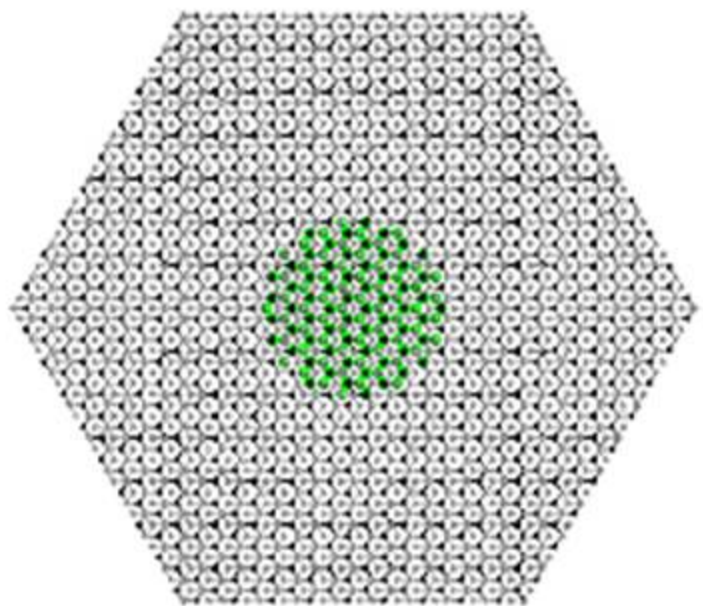
Dose dependence of void and loop radius



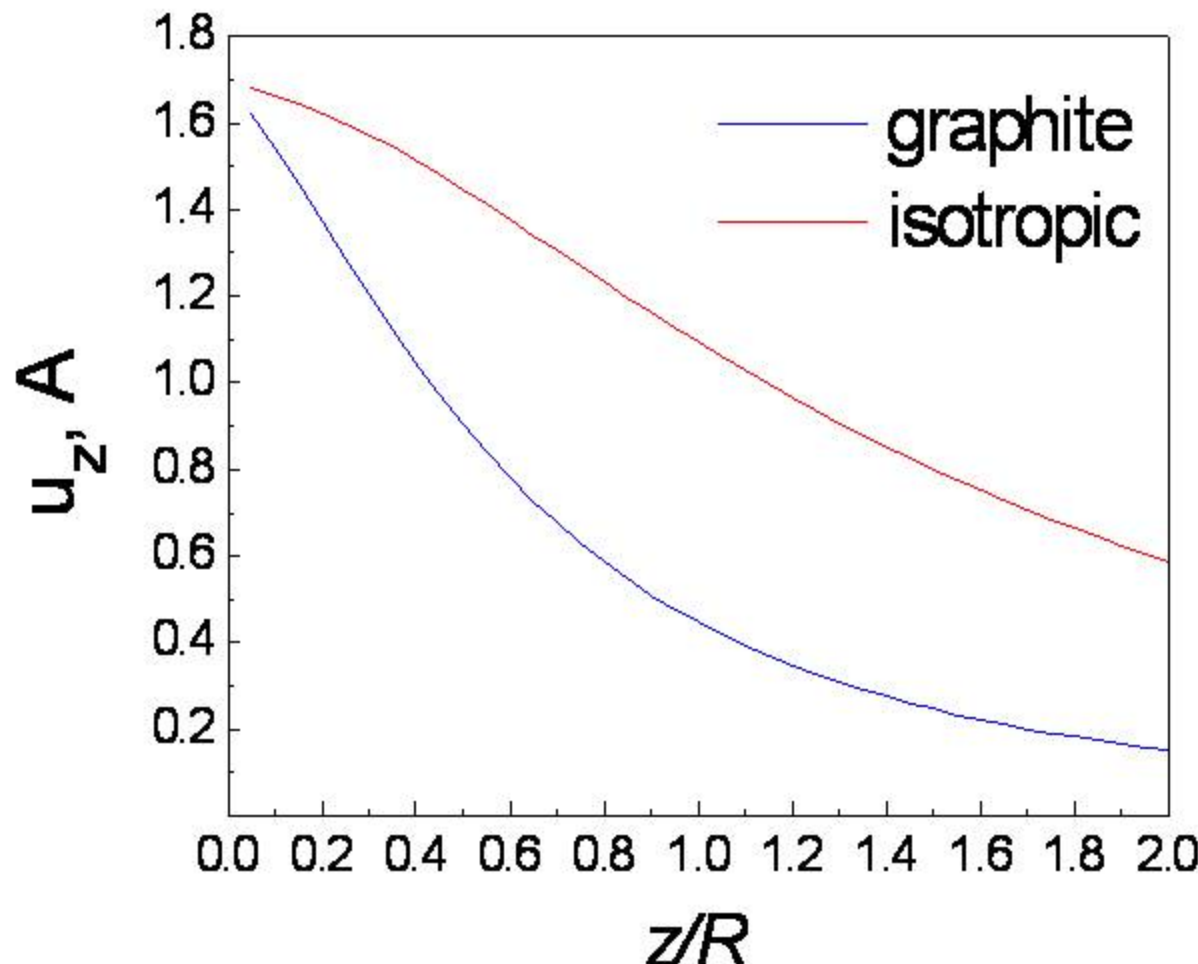
Dose dependence of swelling



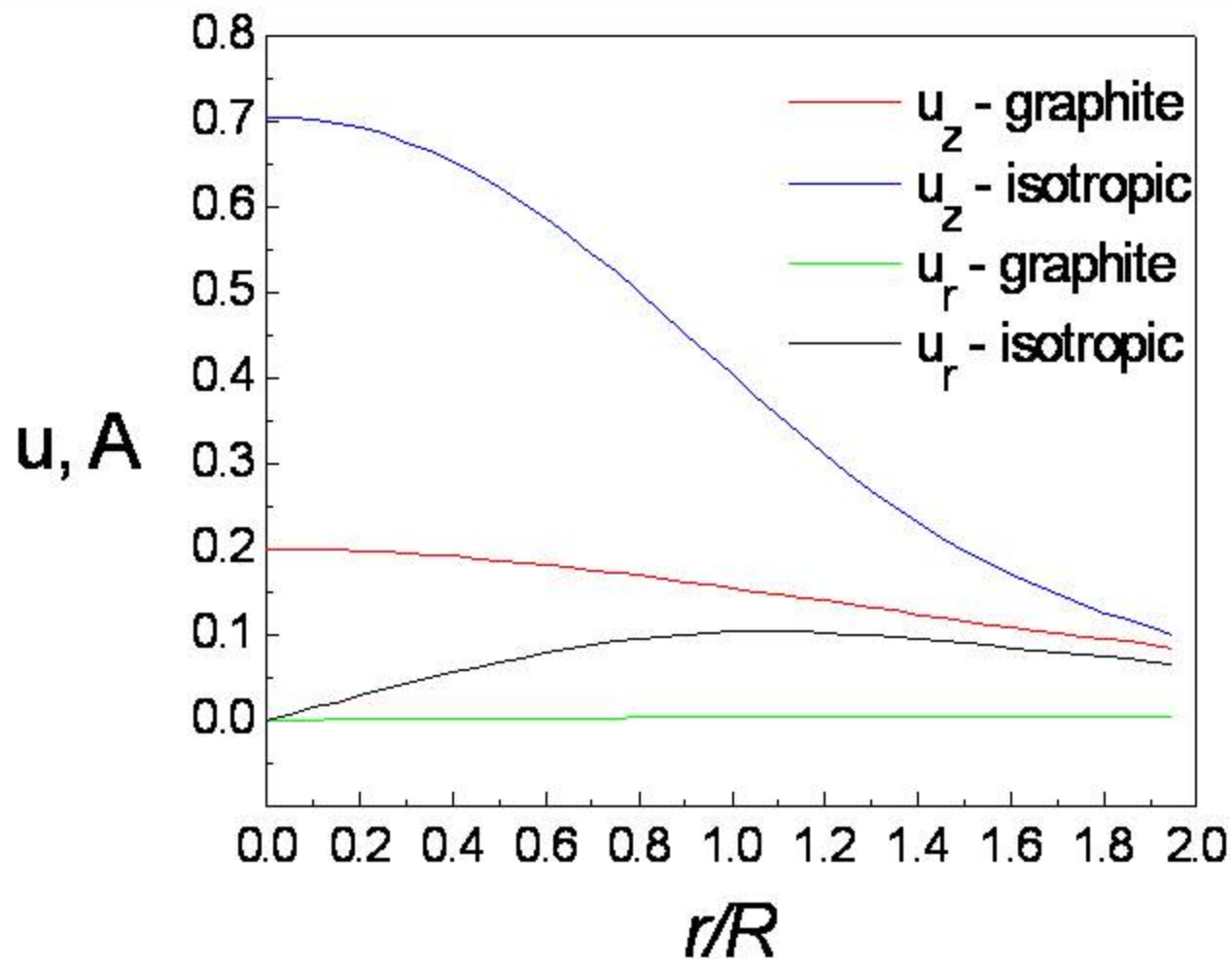
Modeling of dislocation loops in graphite



Distribution of displacement field U_z near dislocation loop in graphite as a function of distance from loop

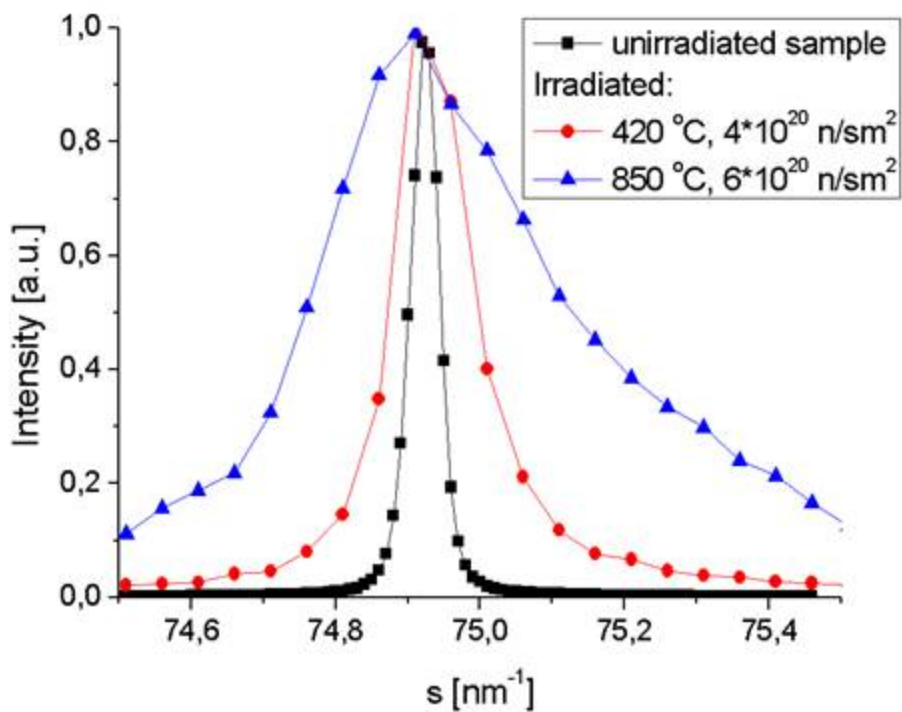


Distribution of vertical and radial displacement field near dislocation loop in graphite as a function of radial distance from loop in basic plane

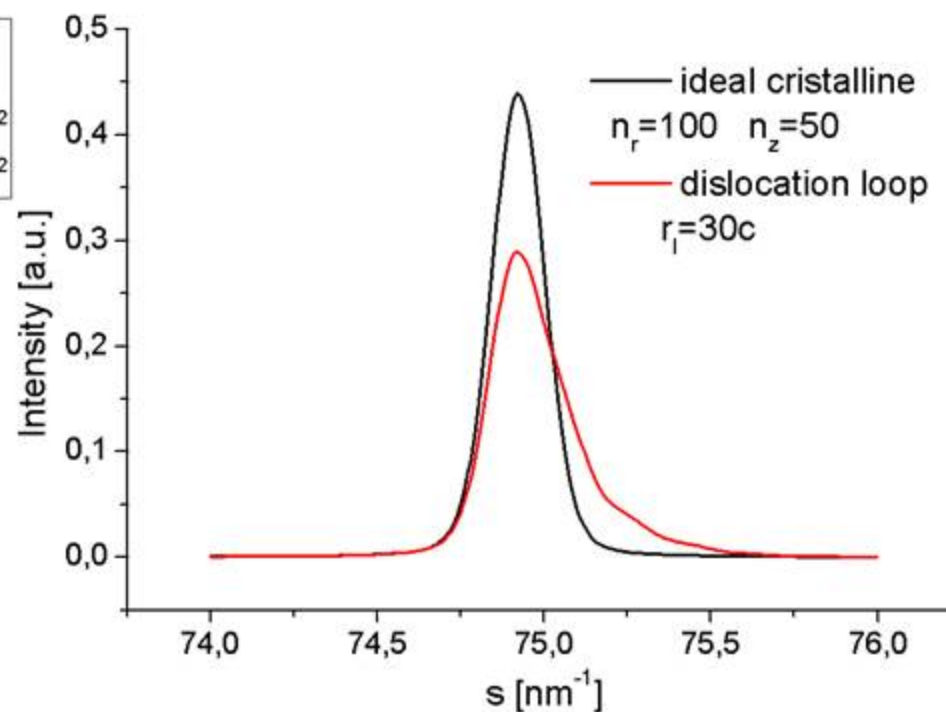


Bragg scattering in irradiated graphite

Experimental Results



Theoretical calculations



EFFECT OF UNDERSIZED SOLUTE ATOMS ON MICROSTRUCTURE CHANGE IN IRRADIATED BINARY VANADIUM ALLOYS

***Russian Research Center “Kurchatov Institute”,
Moscow, Russia**

****Institute for Materials Research, Tohoku University,
Katahira 2-1-1,Aob,Sendai 980-8577, Japan**

Main Aim:

Investigation of dislocation loop formation and growth in irradiated binary V-Fe alloys

Content:

- ◆ Experimental data
- ◆ Physical Model
- ◆ Main Equations
- ◆ Results
- ◆ Comparison theoretical results with experimental data
- ◆ Summary

Experimental Procedure

Materials:

- Pure V (purity 99.9%),
- V-xFe ($x=0.1, 0.2, 0.3, 5$ at%)
- V-yCr ($y=0.1, 1.5$ at%)

Irradiation Facility: *JEM ARM 1250 of HVEM in
Tohoku University, Japan*

Electrons: *Energy up to 1.25 MeV*

Temperature: *from RT to $T = 493$ K,*

Flux of electrons: *4.3×10^{22} to $3.6 \times 10^{23} \text{ e m}^{-2} \text{ s}^{-1}$*

Dose: *Up to $3.36 \times 10^{26} \text{ m}^{-2}$*

Microstructure observations:

*JEM ARM 1250 of HVEM
in Tohoku University, Japan*

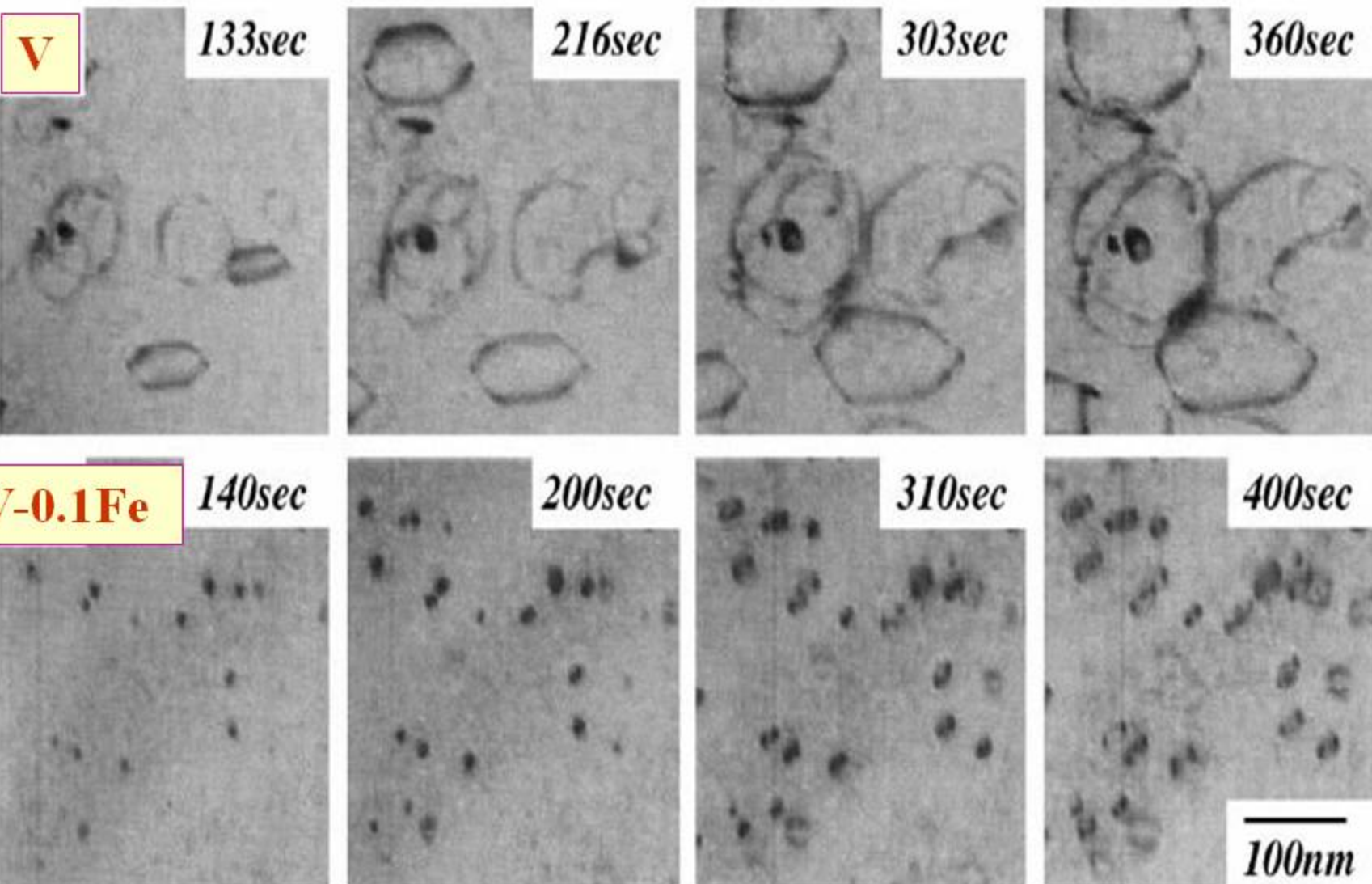
Background

- * Vanadium-based alloys are considered as one of candidate structure materials for fusion reactors
- * Understanding of physical mechanisms of an effect of solute atoms in these alloys on microstructure change is very important for the development of fusion material technology.

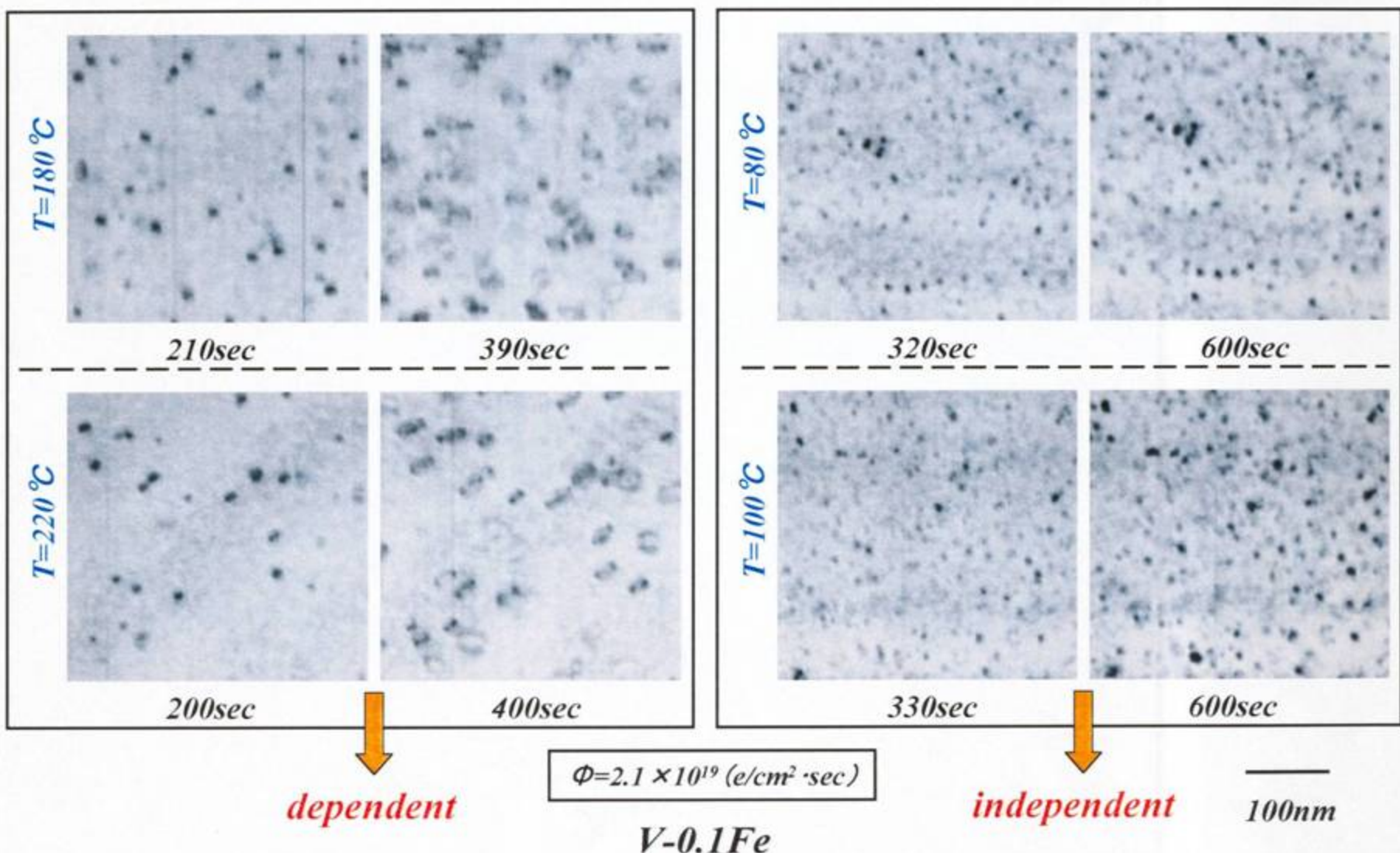
Objective

- Determine the effect of undersized impurity atoms on microstructure change and dislocation loop nucleation and growth in irradiated V-Fe alloys
- Investigation of the dose and temperature dependencies for evolution of dislocation microstructure change in irradiated V-Fe alloys

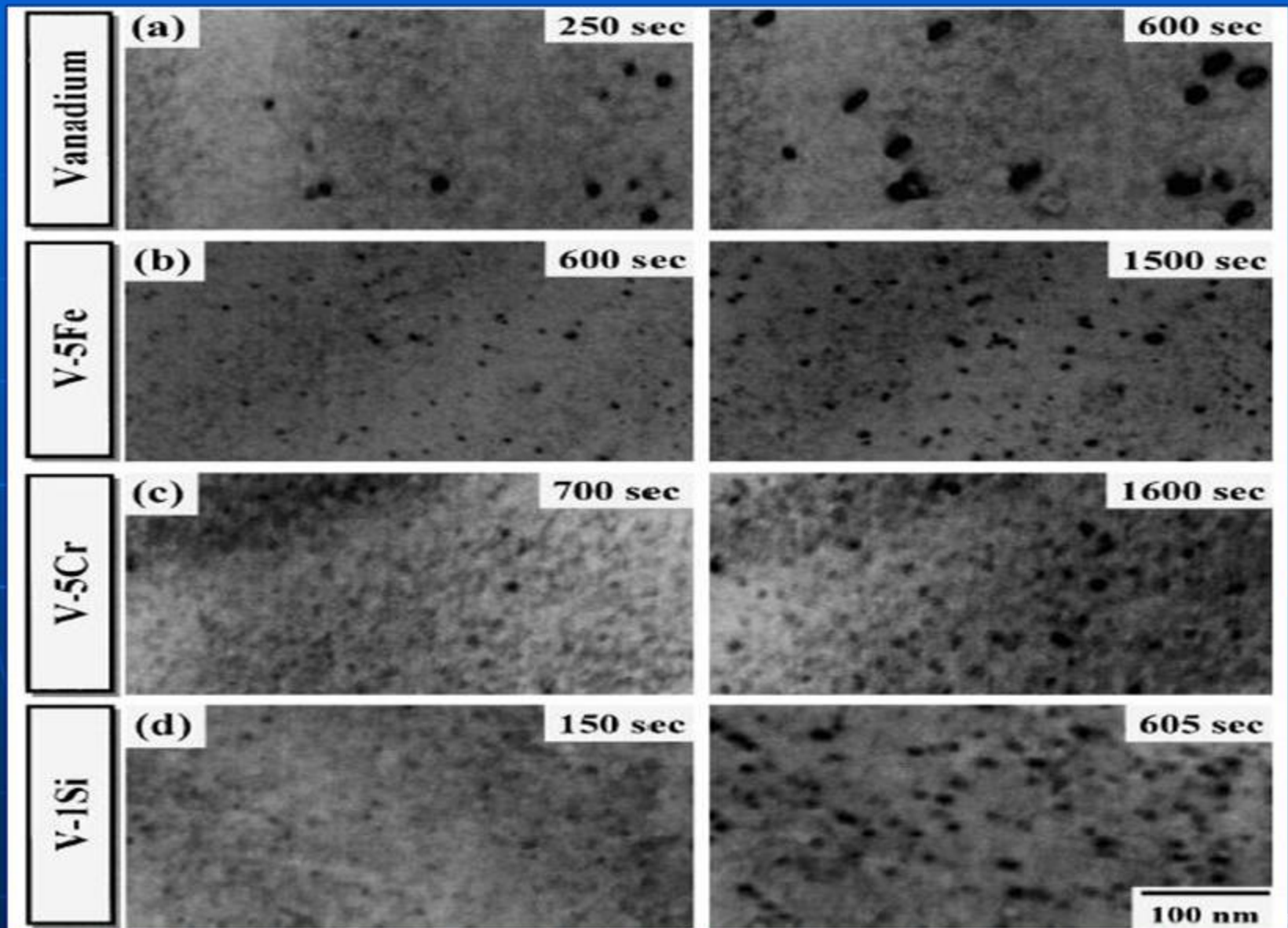
Microstructure evolution in pure V and V-0.1Fe during electron irradiation at T=493K and beam intensity of 2.1×10^{23} e / m² s



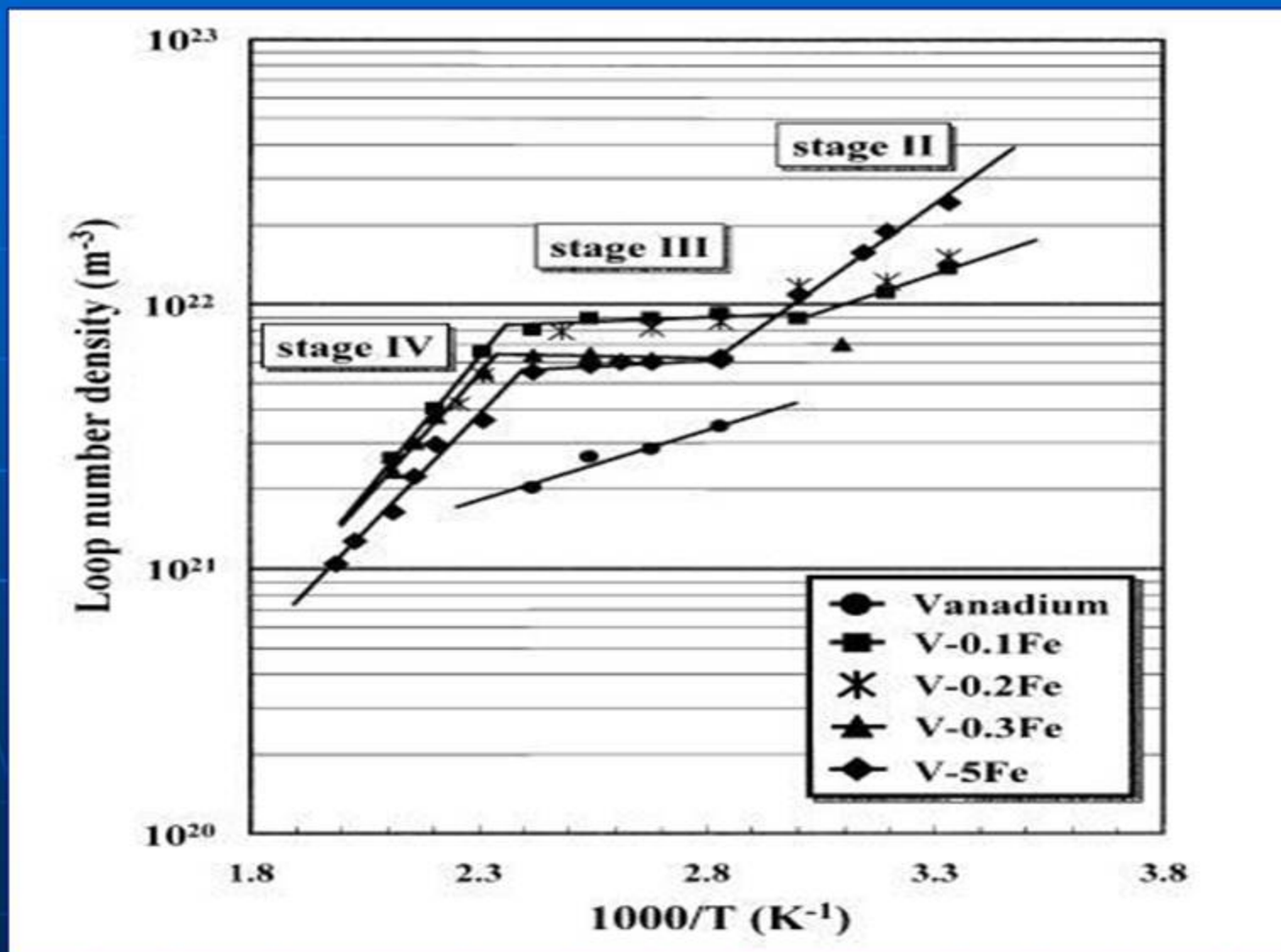
Dependence of loop number density in V-0.1Fe on irradiation temperature



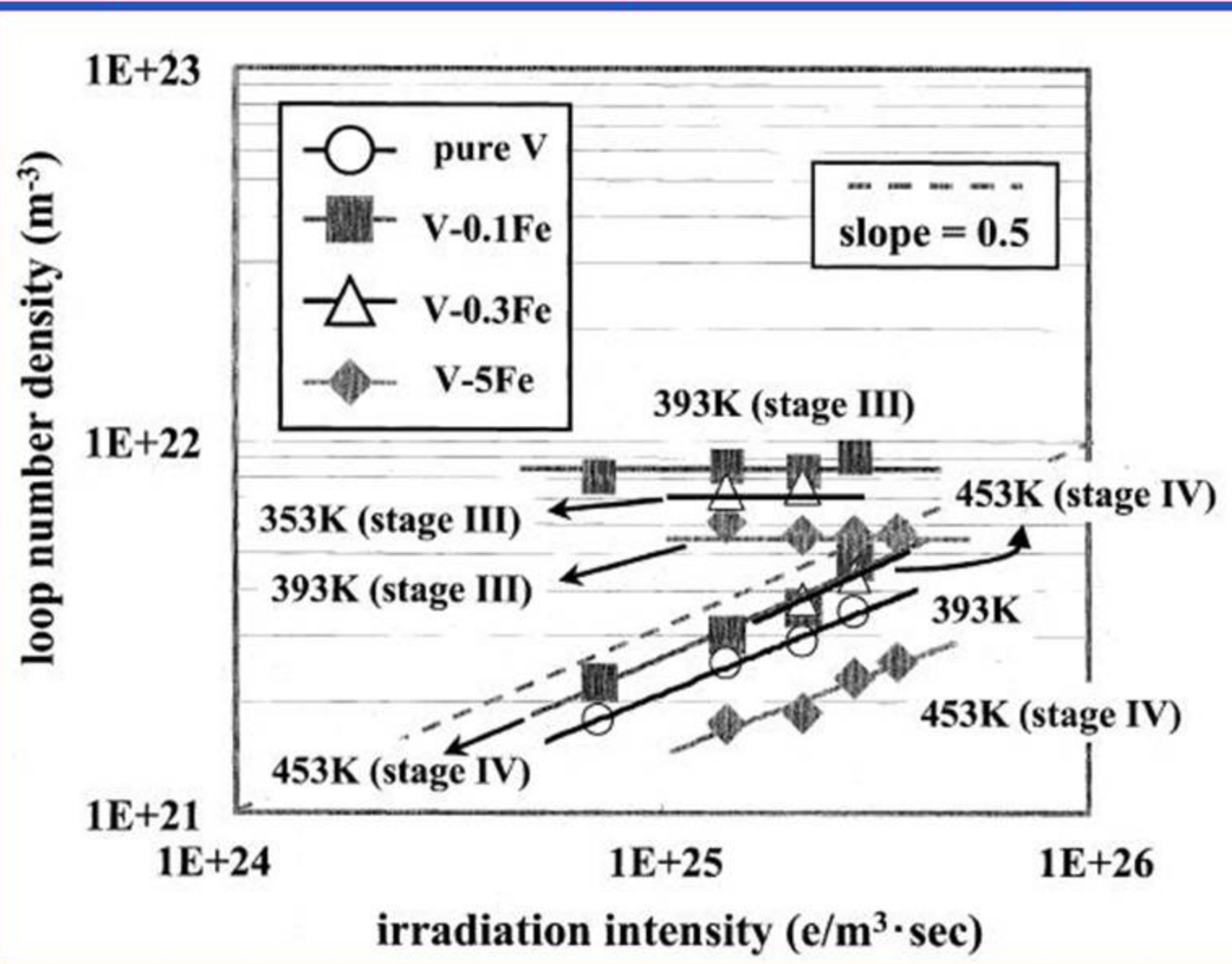
Microstructure change in V, V-5Fe, V-5Cr and V-1Si at electron fluxes: (a)- 1.1×10^{23} em $^{-2}$ s $^{-1}$, (b)-(d) 2.1×10^{23} em $^{-2}$ s $^{-1}$ and T=393 K



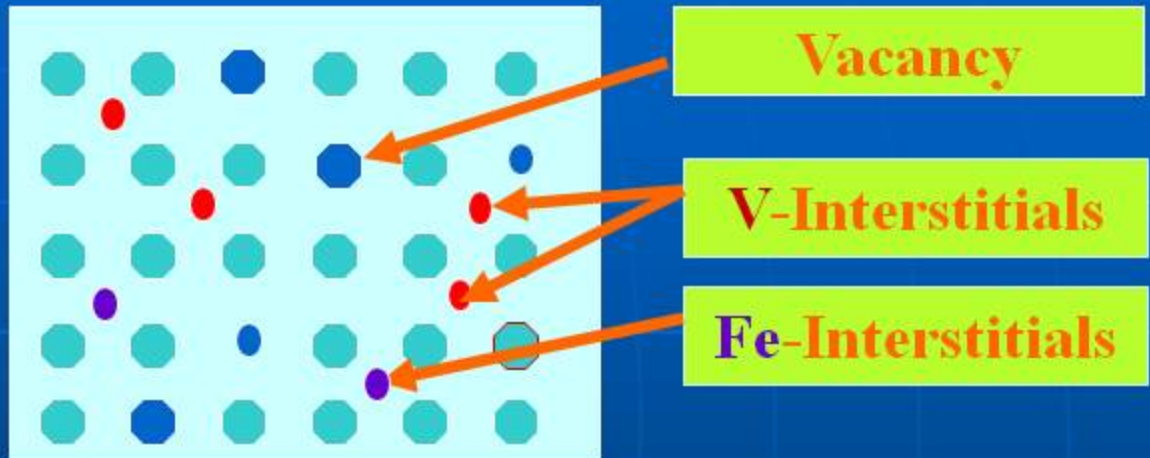
Arrhenius plot of loop number density in V and V-Fe alloys irradiated at electron flux $2.1 \times 10^{23} \text{ em}^{-2}\text{s}^{-1}$



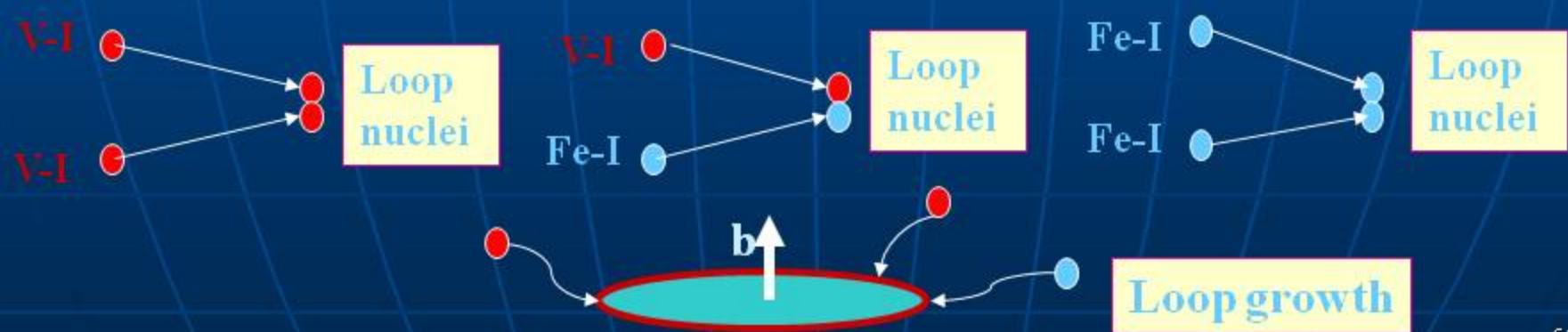
Dependence of loop number density on irradiation intensity in V and V-Fe alloys at various temperatures



Physical Model



Mechanism of dislocation loop nucleation in V-alloys



The system of equations described the nucleation and growth of dislocation loops in irradiated V-alloys

$$\frac{dC_{i1}}{dt} = G_1 - Z_{iv} M_{i1} C_{i1} C_v - Z_{il} (\rho_d + 2\pi R N_l) M_{i1} C_{i1} \alpha^2;$$

$$\frac{dC_{i2}}{dt} = G_2 - Z_{iv} M_{i2} C_{i2} C_v - Z_{il} (\rho_d + 2\pi R N_l) M_{i2} C_{i2} \alpha^2;$$

$$\frac{dC_v}{dt} = (G_1 + G_2) - Z_{iv} (M_{i1} C_{i1} + M_{i2} C_{i2}) C_v - Z_{vl} (\rho_d + 2\pi R N_l) M_v C_v \alpha^2;$$

$$\frac{dN_l}{dt} = Z_{i1} M_{i1} C_{i1}^2 + Z_{i2} M_{i2} C_{i2}^2 + Z_{i1} (M_{i1} + M_{i2}) C_{i1} C_{i2} - \gamma_{12} M_{i1} N_l;$$

$$\frac{dR}{dt} = (Z_{il} (M_{i1} C_{i1} + M_{i2} C_{i2}) - Z_{vl} M_v C_v) \alpha;$$

C_{i1}, C_{i2} and C_v are the concentrations of self interstitials of V atoms, interstitials of Fe atoms and vacancies respectively,

G₁, G₂ are the generation rates of two types of point defects,

M_i, M_v are the mobility of interstitials and vacancies,

a is the lattice spacing ρ_d is the dislocation density,

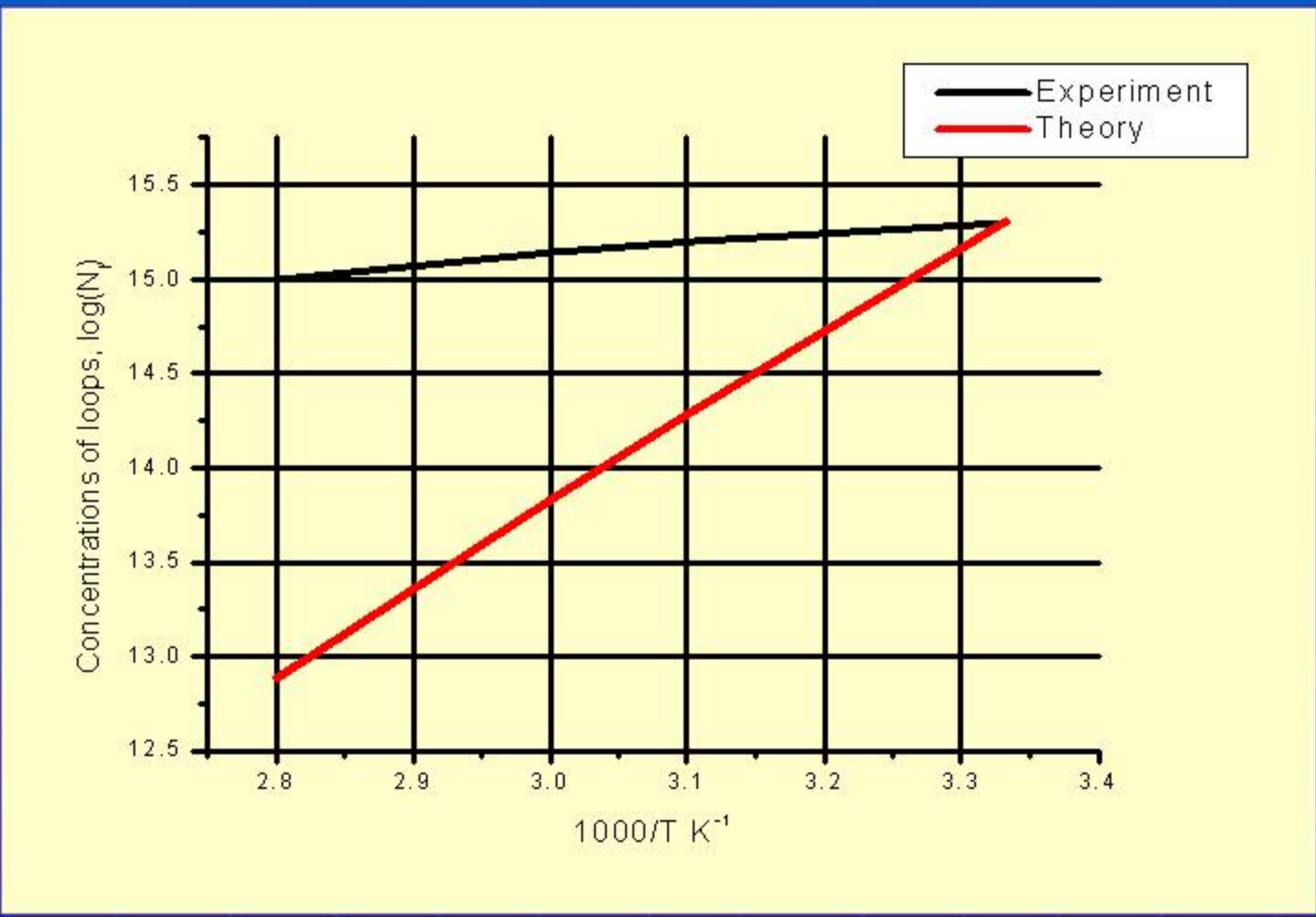
R, N_l are the radius and concentrations of dislocations loops,

Z_{iv}, Z_{il}, Z_{vl}, Z_{ii} are the coefficients which characterize the interaction of point defects between itself and dislocations,

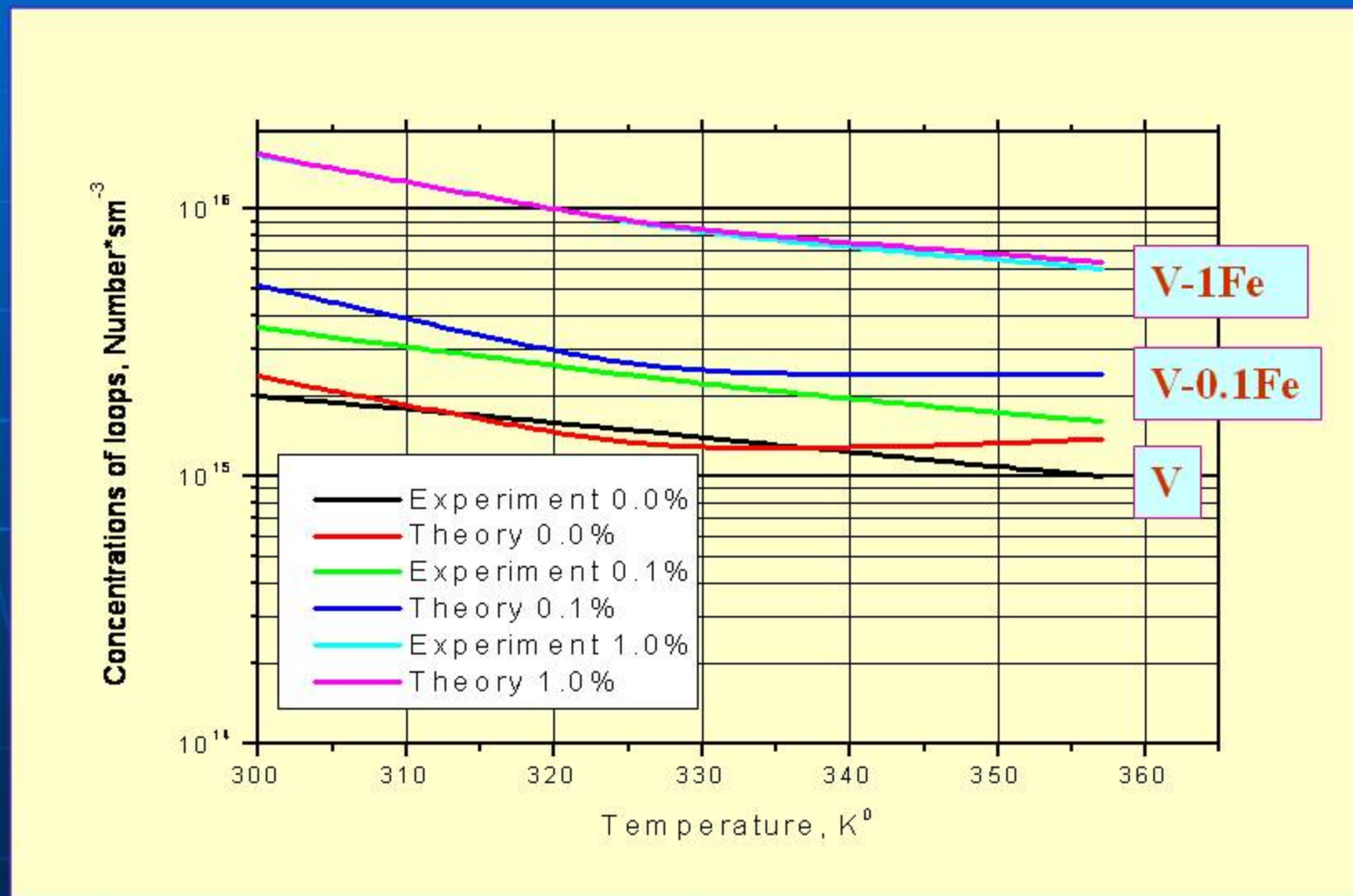
Main values used in numerical loop calculations of dislocation loop formation in irradiated V-Fe alloy

G1	3.31×10^{-4} V sec -1
G2	3.59×10^{-4} Fe sec -1
a	3.03×10^{-8} cm
p	3.13×10^9 cm$^{-2}$
Emi1	0.37 eV
Emi2	0.57 eV
Emv	0.78 eV
Ziv	2.01
Z2i	3.08
Zil	6.25 (T=370K)
Zvl	2.82 (T=370K)

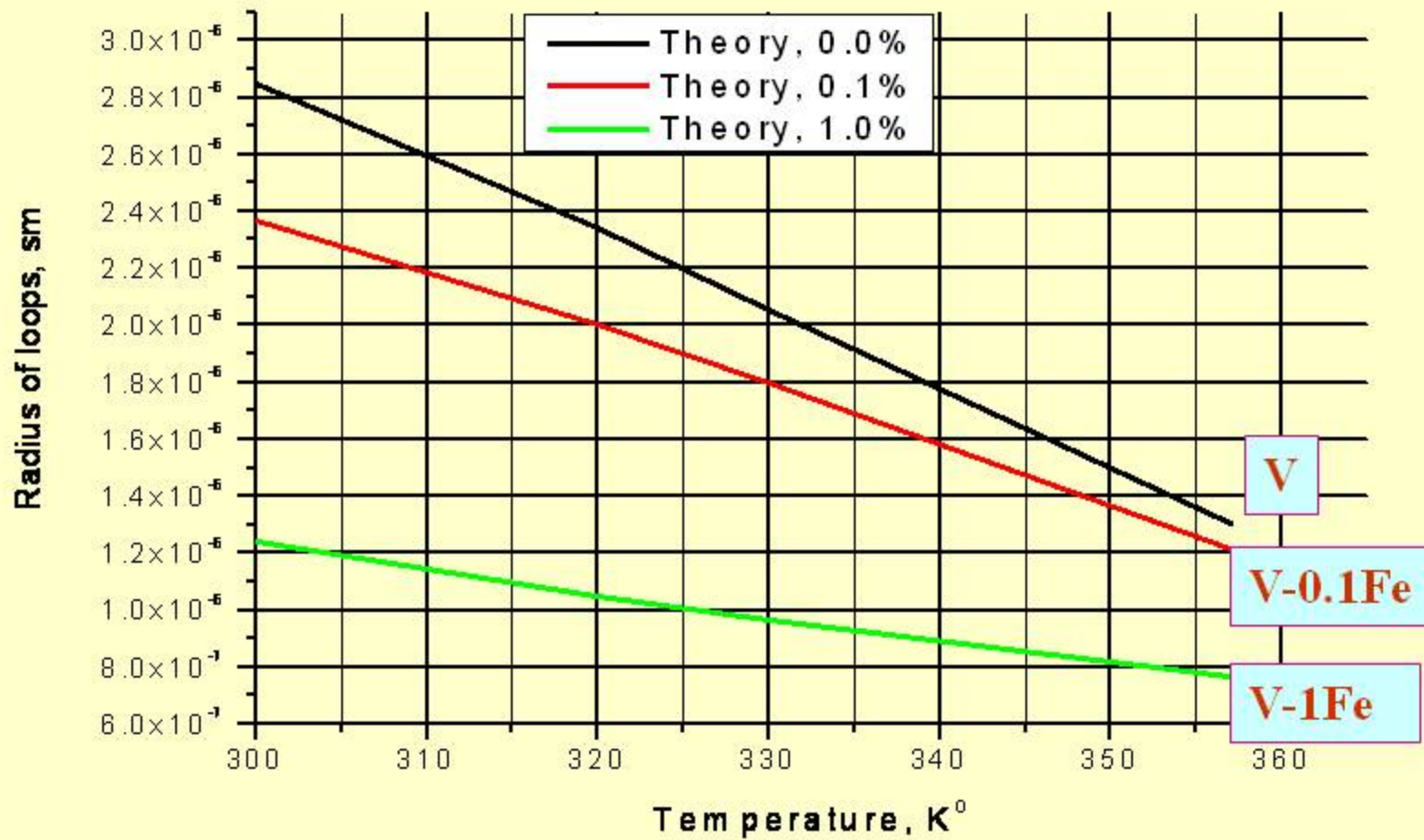
Temperature dependence of dislocation loops density in pure V for experimental and numerical calculations ($\rho d = 1.84 \times 10^{11} \text{ sm}^{-2}$; $E_{mi} = 0.73 \text{ eV}$; $G = 1.9 \times 10^{-4} \text{ dpa/sec}$)



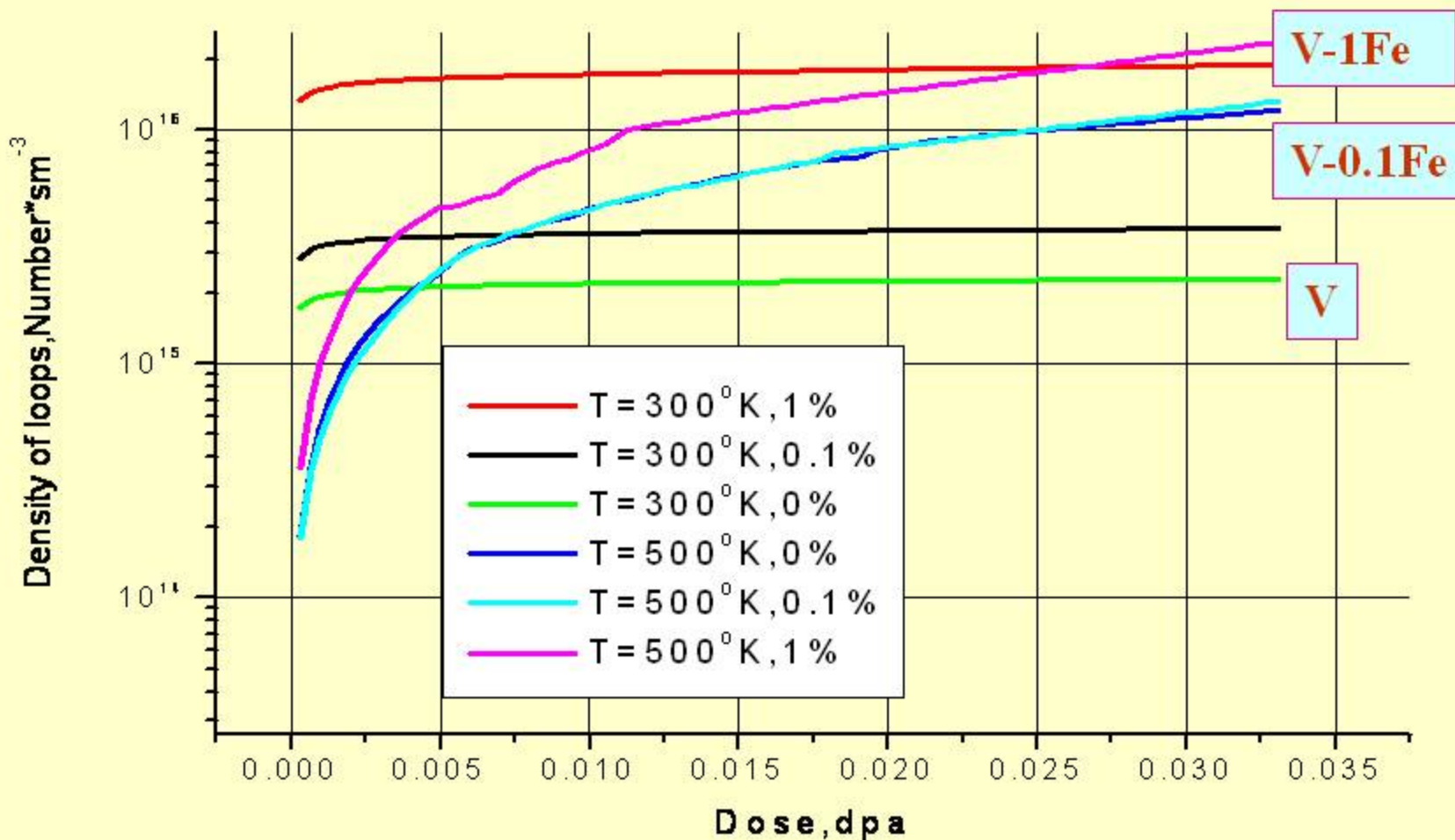
Comparison of experimental results and numerical calculations for temperature dependencies of dislocation loops densities in V-Fe alloys (Pure V, V-0.1Fe and V-1Fe)



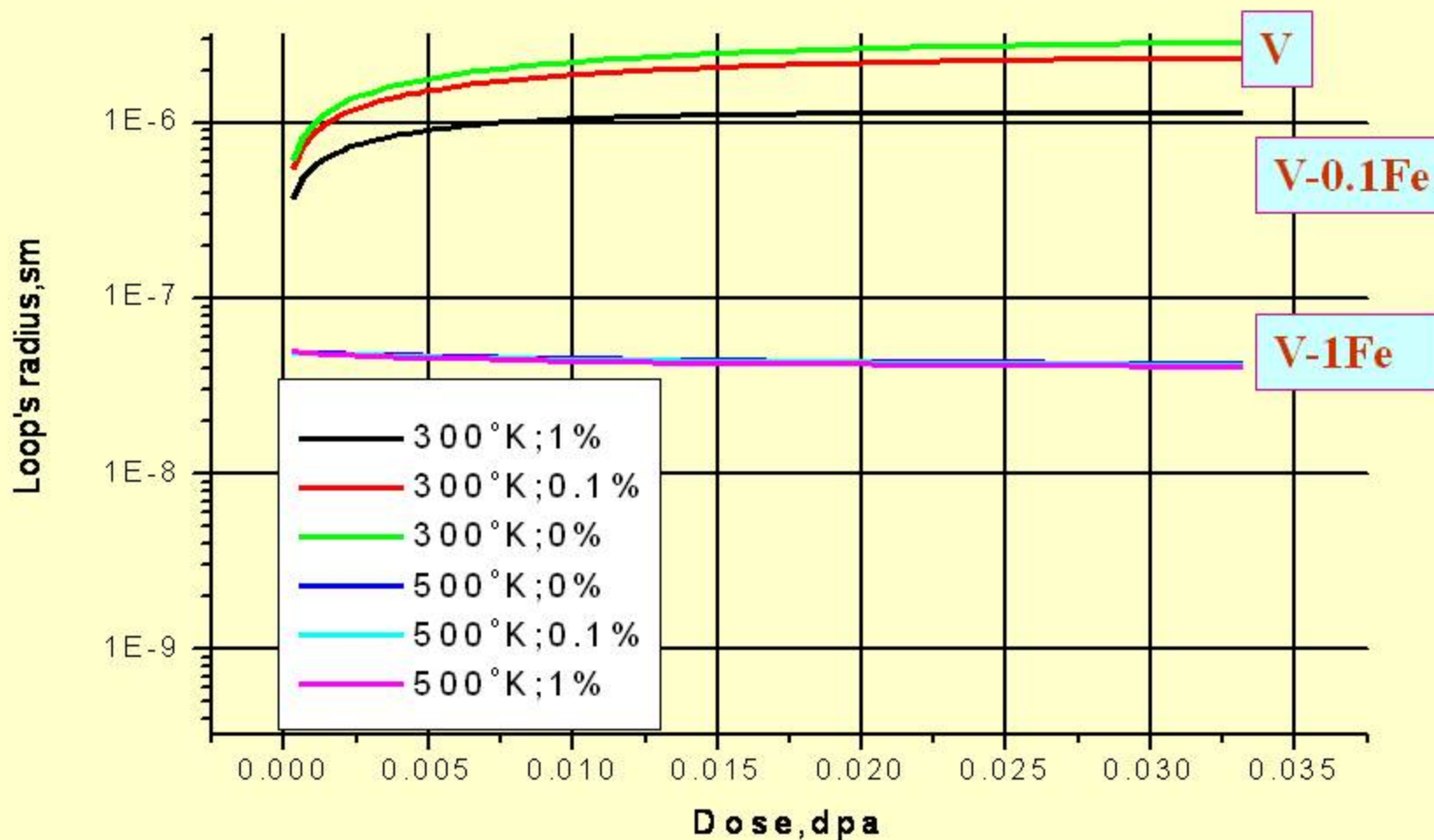
Results of numerical calculations for temperature dependencies of mean dislocation loop radius in V-yFe alloys (Pure V, V-0.1Fe and V-1Fe)



Results of numerical calculations for dose dependencies of dislocation loops densities in V-x Fe alloys (Pure V, V-0.1Fe and V-1Fe) at temperatures: T=300 K and T=500 K



Results of numerical calculations for dose dependencies of mean dislocation loop radius in V-x Fe alloys (Pure V, V-0.1Fe and V-1Fe)



Summary



The microstructure evolution and dislocation loop formation and growth during electron irradiation have been studied by using HVEM and numerical modeling in pure V and V-Fe alloys in a wide range of Fe concentration in order to examine the interaction between V-SIAs and Fe atoms.



Effect of Fe-solutes (undersized atoms) in binary V-Fe alloys on loop nucleation is very significant and dominates the loop nucleation, indicating that Fe-atoms trap V-SIAs and leading to the appearance of the strong temperature dependence.



The theoretical modeling in pure V and V-Fe alloys based on the di-atomic nucleation model of dislocation loops with the migration energies of self interstitial V atoms: $Emi1 = 0.37$ eV and Fe atoms: $Emi2 = 0.57$ eV give the same temperature dependence for dislocation loop density as experimental data.